Advances in Industrial Engineering, December 2026, 60(2): 275-303
DOI: 10.22059/aie.2026.402961.1954

RESEARCH PAPER

Dynamic Analysis of Immune System and Cancer Cell Interactions with an Emphasis on Optimizing Therapeutic Approaches

Maryam Solgi[1], Heibatollah Sadeghi[2*], Amir-Mohammad Golmohammadi[3] and Yazdan Batmani[4]

[1]*Ph.D. Student in Industrial Engineering, University of Kurdistan, Kurdistan, Iran.*
[2]*Associate Professor, Department of Industrial Engineering, University of Kurdistan, Kurdistan, Iran.*
[3]*Associate Professor, Department of Industrial Engineering, Arak University, Arak, Iran.*
[4]*Associate Professor, Department of Electrical Engineering, University of Kurdistan, Kurdistan, Iran.*

Received: 23 September 2025, Revised: 09 May 2026, Accepted: 14 May 2026
© The Author(s) retain the copyright 2026

Abstract

Cancer is a complex and dynamic disease capable of rapidly spreading throughout the body and impairing the immune system. Although immune cells can directly attack tumor cells or activate other components of the immune response, their activity alone is insufficient to achieve complete tumor eradication. Consequently, from a healthcare systems engineering perspective, optimized treatment planning and scheduling are essential to maximize clinical efficacy and resource efficiency. This study employed MATLAB Simulink simulations to model the system dynamics and investigate the effects of chemotherapy and immunotherapy, both individually and in combination, on cancer and immune cells. Cellular population dynamics were first analyzed in the absence of treatment, followed by separate and combined evaluations of each therapy, with particular attention to cellular interactions and cancer cell drug resistance. This approach enables a systematic evaluation of treatment as a multi-objective optimization problem, balancing tumor clearance and immune preservation. The findings revealed that in patients with small initial tumor size and robust immune function, the immune system alone is capable of eliminating cancer cells without therapeutic intervention. However, in patients with large initial tumor size, the combined application of chemotherapy and immunotherapy was predicted to be effective, achieving complete tumor clearance within 38 days while preserving overall health. Collectively, the simulation results suggest that combined chemo-immunotherapy, especially when the sequence of administration is carefully considered, is predicted to be the most effective strategy among the tested protocols and may serve as a model-based decision support tool for personalized healthcare management, pending prospective clinical validation.

Keywords:
Cancer Treatment, Combination Therapy, Drug Resistance, Healthcare Systems Engineering, System Dynamics Simulation.

1. Introduction

Cancer is one of the most complex human diseases, which, due to its dynamic and multifaceted nature, establishes diverse interactions with the immune system. Cancer cells have the ability to evade the defense mechanisms of the immune system[1-3]. Despite significant advances in

* Corresponding author: (Heibatollah Sadeghi)
Email: h.sadeghi@uok.ac.ir

cancer treatment, including chemotherapy, radiotherapy, and immunotherapy, numerous challenges remain[4]. Chemotherapy, as one of the primary cancer treatment modalities, targets cancer cells but also damages healthy cells and is associated with side effects. Moreover, during the course of treatment, the emergence of both innate and acquired drug resistance remains a major obstacle, with over 90% of therapeutic failures in metastatic cancers linked to multi-drug resistance (MDR) mechanisms [5]. On the other hand, immunotherapy, designed to enhance the immune system, is in some cases insufficient on its own to control the growth of large or advanced tumors and has limited efficacy in eradicating cancer cells alone due to tumor heterogeneity and an immunosuppressive tumor microenvironment (TME) [6, 7]. This underscores the necessity of employing combination therapeutic approaches [8, 9].

While chemotherapy is a cornerstone of treatment, recent evidence indicates that its combination with immune checkpoint inhibitors (ICIs) can produce synergistic effects. For instance, in extensive-stage small cell lung cancer (SCLC), the addition of atezolizumab or durvalumab to platinum-etoposide chemotherapy has been shown to improve overall survival (OS) compared to chemotherapy alone [7]. Similarly, in non-small cell lung cancer (NSCLC), pembrolizumab combined with chemotherapy has demonstrated superior outcomes over chemotherapy alone, establishing new first-line standards [7]. However, recent studies have shown that combining chemotherapy with immune enhancers can improve therapeutic efficacy and help overcome drug resistance [10].

A critical challenge in current cancer therapy is the ability of tumors to develop resistance not only to chemotherapy but also to novel immunotherapies, including ICIs [11, 12]. In metastatic castration-resistant prostate cancer (mCRPC), resistance to taxanes, androgen receptor signaling inhibitors (ARSIs), and PARP inhibitors arises through mechanisms such as tubulin mutations, AR splice variants (e.g., AR-V7), and reversion mutations in HRR genes [11]. Furthermore, in the context of ICIs, resistance is frequently driven by an immunosuppressive TME characterized by regulatory T cells (Tregs), myeloid-derived suppressor cells (MDSCs), and defects in antigen presentation machinery [13].

The key focus of this study is the analysis and modeling of the dynamic interactions between immune cells and cancer cells to improve the efficacy of combination therapies. The objective is to develop a comprehensive mathematical model to evaluate the effects of various treatments, including chemotherapy, immunotherapy, and their combination, on tumor growth and immune system behavior. This model is designed to account for factors such as drug resistance, the cytotoxic effects of therapies on the immune system, and the role of various biological parameters.

a) Based on the literature review, the following challenges have been identified in this field:
   a. Achieving a precise understanding of the interactions between the immune system and cancer cells.
b) Accounting for the impact of drug resistance on treatment efficacy.
c) Simulating the behavior of the immune system and tumors in the presence of combination therapies.
d) Developing optimization strategies to minimize side effects and enhance treatment effectiveness.

This study is designed to accurately model biological interactions and simulate the effects of combination therapies, aiming to provide a comprehensive response to the identified challenges. The results of this research can contribute to the development of optimized and personalized treatment protocols for cancer patients, while also serving as a foundation for future studies in the field of innovative cancer therapies.

This study adopts an industrial engineering perspective by applying systems modeling and simulation methodologies to a critical healthcare problem. Healthcare systems engineering, as an important subfield of industrial engineering, utilizes tools such as mathematical modeling,

simulation, and optimization to analyze complex systems, improve decision-making, and enhance the efficiency and effectiveness of healthcare delivery. In this context, the present research employs MATLAB Simulink and ordinary differential equation (ODE)-based dynamic modeling to simulate the interactions between cancer cells and the immune system. This approach enables systematic evaluation and optimization of treatment strategies, contributing to the broader field of operations research and systems engineering in healthcare.

One of the key aspects of combating cancer is achieving a precise and in-depth understanding of the interactions between cancer cells and the immune system, as these interactions significantly influence tumor growth and the body's response to treatment. In this regard, numerous scientific studies have been conducted to examine the interactions between immune cells and cancer cells.

Shu et al. [14] developed a mathematical model of tumor-macrophage interactions using a logistic growth function. A key strength of their work was the sensitivity analysis identifying parameter importance; however, a major limitation was the omission of drug resistance mechanisms and adaptive immune components (CD8+ T cells), which are crucial for evaluating modern immunotherapies such as ICIs. Pang et al. [15] presented a mathematical model of tumor growth dynamics incorporating the effects of radiotherapy. This study examined how the reoxygenation of hypoxic cells and radiotherapy sensitivity influence treatment outcomes. The results indicated that higher radiotherapy sensitivity coefficients and increased tumor cell reoxygenation enhance the effectiveness of radiotherapy. Ghaffari et al. [16] compared six classical tumor growth models using clinical data from 1,472 patients. While the Gompertz model offered the best balance of accuracy and parsimony, a significant weakness of their approach was the lack of mechanistic immune components, limiting its ability to predict responses to combination chemo-immunotherapy or explain resistance driven by the TME.

Sung et al. [17] proposed a mathematical model based on the dynamic biological interactions between the immune system and tumors, using input data from patient blood samples and clinical test results. The presented model comprises four ordinary differential equations representing the growth of tumor cells and circulating lymphocytes. In this study, tumor cells were categorized into three groups: the first group consists of tumor cells exposed to radiation, the second group includes cells not exposed to radiation, and the third group comprises inactivated tumor cells. Additionally, the effect of immune checkpoint inhibition (ICI) was incorporated into the model using an immune activation term. However, a notable weakness of Sung's model is that it does not differentiate between drug-sensitive and drug-resistant tumor cells, a distinction now recognized as critical for capturing acquired resistance dynamics [5]. Kim et al. [18] extended Sung's model by incorporating the effect of protein 4 associated with cytotoxic T lymphocytes (CTLA-4). Simulations from the proposed model can predict patient responses to the combined effect of CTLA-4 and radiotherapy. The results indicate that administering CTLA-4 prior to radiotherapy is beneficial in terms of treatment sequencing. Nevertheless, this extension did not account for other key immunosuppressive populations such as MDSCs or Tregs, which have been shown to substantially attenuate ICI efficacy [6].

Bitsouni et al. [19] provided one of the more comprehensive models by including multiple immune populations (NK, CD4+, CD8+, Tregs, B cells) and chemotherapy. A major strength was the experimental validation showing NK cell elimination follows a ratio-dependent functional response. However, their model did not incorporate the impact of drug resistance or the sequencing of combination therapies, which are central to optimizing clinical protocols [11, 20].

Mahasa et al. [21] addressed the key question of whether single or multiple sequential doses of chimeric antigen receptor T (CAR-T) cells, combined with oncolytic viruses (OVs) during treatment, can produce a synergistic effect in tumor reduction. To investigate this, they

developed an ordinary differential equation (ODE)–based model incorporating synergy from OVs to evaluate the potential effects of different regimens that could lead to an effective combined therapy against tumor cell populations. Model simulations indicate that while a single CAR-T dose alone is insufficient to eradicate all tumor cells, combining the same CAR-T dose with a single OV dose can successfully eliminate the tumor even in the absence of virus-induced synergy. A key limitation of this study, however, is the absence of an immunosuppressive TME component, which is known to significantly hinder CAR-T cell infiltration and persistence in solid tumors [20].

Shariatpanahi et al. [22] made a significant contribution by explicitly modeling MDSCs, a key mediator of immune suppression. The model's strength lies in its validation against experimental data on MDSC expansion and recovery with 5-FU. However, the framework did not include the dynamics of PD-1/PD-L1 checkpoint interactions, which are now a major target of modern immunotherapy and a known driver of T cell exhaustion [13].

Owens and Bozic [23] simulated combination chemotherapy and CAR-T therapy using an ODE model and performed sensitivity analysis, revealing that small improvements in CAR-T cytotoxic effectiveness significantly reduce the required therapeutic dose. A strength was the alignment of simulation results with clinical observations on preconditioning. However, their model did not include the effects of the TME or tumor heterogeneity, which are primary barriers to CAR-T success in solid tumors [20]. In summary, while previous models have advanced our understanding of tumor-immune dynamics, several critical gaps remain: (1) Most models do not simultaneously account for drug-sensitive and drug-resistant tumor cell populations, despite the central role of MDR in treatment failure [5, 12]. (2) The immunosuppressive roles of Tregs and MDSCs, which are key targets for overcoming ICI resistance, are frequently omitted or oversimplified [6, 13]. (3) Many models focus on monotherapy (e.g., chemotherapy alone or ICI alone) and do not systematically evaluate the optimal sequencing and combination of chemo-immunotherapy to minimize immune toxicity while maximizing tumor clearance [11, 16]. (4) Quantitative comparisons of treatment protocols (e.g., concurrent vs. sequential vs. pulsed administration) and their impact on both tumor size and immune cell preservation are lacking in the literature.

This background highlights the need for a comprehensive model that incorporates key biological factors and examines the effects of various combination therapies. Such modeling should not only assess the direct effects of treatments on tumor cell growth but also take into account the underlying role of the immune system and the interactions among its different components. Accordingly, this study proposes a mathematical model that considers the interactions between tumor and immune cells to investigate the impact of chemo-immunotherapy. A distinctive feature of this modeling is the inclusion of immunosuppressive cells along with their stimulatory factors. Furthermore, accounting for drug resistance and evaluating different therapeutic strategies are additional aspects that distinguish this research from previous studies. Thus, the innovations of the paper can be categorized as follows:

a) Comprehensive modeling of interactions between immune cells and tumor cells including both stimulatory and inhibitory (Tregs, MDSCs) arms.
b) Simulation of combination therapies aimed at achieving optimal treatment with quantitative comparison of concurrent, sequential, and pulsed protocols
c) Consideration of different conditions for personalized therapy
d) Introduction of new variables such as drug-resistant tumor subpopulations and immune cell toxicity
e) Proposal of various protocols for combining immunotherapy and chemotherapy

In this article, the introduction and literature review provide a comprehensive overview of various cancer treatment methods, interactions between immune cells and tumor cells, and related previous studies. In the mathematical modeling section, the proposed model for the

interactions between immune cells and tumor cells is presented in detail along with its parameters and equations. The simulation methodology section includes the details of the simulations and the methods employed in MATLAB Simulink for implementing the model. In the results analysis, the simulation outcomes for different therapeutic approaches and various combinations are presented and analyzed. In the conclusion and recommendations, the scientific and practical contributions of the study are discussed, along with suggestions for future research. Finally, the references section includes the list of sources and articles used.

In order to evaluate the biological consistency of the proposed model, the simulation results were compared with publicly available clinical data reported by Ghaffari et al. [16]. Their study provided longitudinal tumor volume measurements from 1,472 cancer patients with at least three measurements per target lesion. The data were collected from five clinical trials in which patients with non-small cell lung cancer and bladder cancer received either atezolizumab (immunotherapy) or docetaxel. Compared to previous mathematical models of tumor-immune dynamics, the present study offers several methodological distinctions. While Kirschner and Panetta [9] focused on IL-2 immunotherapy alone and Ghaffari et al. [16] provided clinical validation using simplified growth models without mechanistic immune components, the proposed model simultaneously incorporates drug-sensitive and drug-resistant tumor populations, multiple immune cell types (NK, $CD4^+$, $CD8^+$, and circulating lymphocytes), IL-2 dynamics, and combination chemo-immunotherapy with optimized sequencing. This integrated approach allows quantitative comparison of treatment strategies that has not been previously reported. The main novelty of the present study lies in the systematic evaluation of treatment sequencing on both tumor clearance and immune cell preservation, as well as the identification of sensitive parameters through comprehensive sensitivity analysis.

2. Problem Description

The present study focuses on modeling the complex interactions between cancer cells and the immune system, with the aim of developing an optimized combination therapy regimen involving chemotherapy and immunotherapy. In the proposed model, cancer cells are categorized into drug-sensitive and drug-resistant populations, reflecting the clinical reality that a subset of tumor cells acquires resistance over time, thereby reducing treatment efficacy. This classification enables a precise assessment of the impact of drug resistance on tumor progression and therapeutic response, a factor often neglected in previous studies.

To achieve a realistic simulation of immune system dynamics, the model incorporates circulating lymphocyte populations and CD4+ T cells, providing a comprehensive representation of immune-tumor interactions beyond the basic factors typically considered in prior models.

The primary objective of this research is to optimize therapeutic strategies, including both combination and monotherapy approaches, based on patient-specific biological characteristics.

The model systematically evaluates whether monotherapies (chemotherapy or immunotherapy) or combination therapies produce superior tumor control and immune response. Moreover, it examines the temporal sequencing of treatments and dosing schedules to determine the optimal therapeutic regimen.

Key innovations of this study include:

- Classification of cancer cells into drug-sensitive and drug-resistant populations, with simulation of transitions to resistance.
- Incorporation of clinically relevant immune factors, including circulating lymphocytes and $CD4^+$T cells, enabling a more accurate representation of immune-tumor dynamics.
- Optimization of combination therapy strategies and comparative evaluation against monotherapies, including analysis of treatment sequencing and dosing schedules to

determine patient-specific optimal regimens.

This approach enables precise simulation of the body's response to therapy, supports the design of personalized treatment strategies, and establishes a robust foundation for future investigations into novel combination therapies.

3. Mathematical Modeling

The problem addressed in this study is the mathematical modeling of interactions between cancer cells and immune cells, aiming to gain a deeper understanding of tumor growth dynamics and the role of various factors in this process. This research examines the changes in cell populations under different treatment strategies. For this purpose, six cellular populations are considered: drug-sensitive tumor cells, drug-resistant tumor cells, natural killer (NK) cells, $CD8^{+}T$ cells, $CD4^{+}T$ cells, and other circulating lymphocytes. To represent the interactions between tumor cells and immune cells within the tumor microenvironment, as well as the effects of therapeutic interventions, the following model is proposed:

$$\frac{dS}{dt} = aS(1 - bS) - c_n NS - DS - \frac{p_1 S\, I}{g_1 + S} - lS - K_S(1 - e^{-M})S \tag{1}$$

$$\frac{dR_1}{dt} = aR_1(1 - bR_1) - c_n NR_1 - DR_1 - \frac{p_1 R_1\, I}{g_1 + R_1} + lS \tag{2}$$

$$\frac{dN}{dt} = e_3 C - f_2 N + \frac{g_3 N T^2}{g_4 + T^2} - p_a TN - K_N(1 - e^{-M})N \tag{3}$$

$$\frac{dL}{dt} = -m_1 L + \frac{J_3 D^2 T^2}{K_3 + D^2 T^2} L - q_l LT + (r_3 N + r_4 C)T - u_2 L^2 N + \frac{P_I LI}{g_I + I} - K_L(1 - e^{-M})L + V_l(t) \tag{4}$$

$$V_l(t) = \begin{cases} 0 & \text{if } t \notin \text{injection times} \\ \omega & \text{if } t \in \text{injection times} \end{cases}$$

$$\frac{dY}{dt} = -\mu_1 Y + \frac{\beta_1\, T}{\alpha_1 + T} I - \delta_2 TY \tag{5}$$

$$\frac{dC}{dt} = \alpha_C - \beta_C C - K_C(1 - e^{-M})C \tag{6}$$

$$\frac{dM}{dt} = -\gamma_M M + U_M(t) \quad , \quad U_M(t) = \begin{cases} 0 & \text{if } t \notin \text{injection times} \\ \sigma & \text{if } t \in \text{injection times} \end{cases} \tag{7}$$

$$\frac{dI}{dt} = -\mu_I I + \frac{\beta_2 TY}{\alpha + T} + V_I(t) \quad , \quad V_I(t) = \begin{cases} 0 & \text{if } t \notin \text{injection times} \\ \delta & \text{if } t \in \text{injection times} \end{cases} \tag{8}$$

$$D = d\frac{(\frac{L}{T})^{l_2}}{o + (\frac{L}{T})^{l_2}}$$

Equation (1) represents the growth dynamics of treatment-sensitive tumor cells. The first term is a logistic function used to describe tumor cell proliferation. The second term accounts for tumor cell elimination due to interactions with natural killer (NK) cells. The third term represents the effect of $CD8^{+}T$ cells on tumor cells. The fourth term describes the impact of interleukin-2 (IL-2) on tumor cell destruction. The fifth term indicates the number of sensitive cells that convert into resistant cells over time, and the last term represents the effect of chemotherapy on tumor cells. Equation (2) represents the growth dynamics of treatment-resistant tumor cells. The first term is a logistic function used to describe tumor cell proliferation. The second term accounts for interactions between natural killer (NK) cells and tumor cells. The third term represents the effect of $CD8^{+}T$ cells on tumor cells. The fourth term

describes the impact of interleukin-2 (IL-2) on tumor cells, and the fifth term indicates the number of sensitive cells that convert into resistant cells.

Equation (3) represents the dynamics of natural killer (NK) cell populations. These cells exist in the body even in the absence of a tumor and are part of the circulating lymphocytes, which is reflected in the first term. The second term represents the natural death of NK cells. The third term describes the stimulation and activation of NK cells in response to the presence of tumor cells. The fourth term accounts for the interactions between NK cells and tumor cells, and the last term represents the effect of chemotherapy on NK cells.

Equation (4) represents the dynamics of $CD8^+$T cells. It is assumed that no $CD8^+$T cells exist in the absence of tumor cells, so tumor cells are the source of their activation. The first term represents the natural death of $CD8^+$T cells. The second term denotes the recruitment of $CD8^+$T cells due to the presence of tumor cells. The third term represents $CD8^+$T cell death resulting from interactions with tumor cells. The term r_1NT indicates the stimulation of $CD8^+$T cells by the remnants of tumor cells destroyed by NK cells, while r_2CT represents the activation of $CD8^+$T cells within the general lymphocyte population. The sixth term describes the regulation and suppression of CD8+T cell production by NK cells, which occurs when very high levels of active $CD8^+$T cells are present. Cytokine-induced activation of $CD8^+$T cells is represented by $(p_i\, I/\, (g_i + I))\, L$. The next term shows the effect of chemotherapy on $CD8^+$T cells, and the last term represents an external source of $CD8^+$T cells.

The changes in the population of $CD4^+$T cells are described by equation (5), which includes a constant death rate μ_1\mu$_1$. The second term in this equation represents the effect of cytokine activation on $CD4^+$T cells due to the presence of tumor cells. The third term shows the loss of these cells as a result of interactions with the tumor.

Equation (6) represents the population of circulating lymphocytes, which are assumed to be produced at a constant rate α_C and undergo death at a rate β_C. The last term in this equation indicates the effect of chemotherapy on circulating lymphocytes. Equation (7) represents the changes in the concentration of chemotherapy drugs in the body. The first term indicates the rate of drug elimination from the bloodstream of the patient, while the term $U_M(t)$represents the external source of chemotherapy, in other words, it denotes the therapeutic protocol used for chemotherapy. Equation (8) represents the changes in the concentration of IL-2 cytokine in the body. The first term indicates the rate of IL-2 elimination from the body, while the term $V_I(t)$ represents the external source of interleukin-2, in other words, it denotes the therapeutic protocol used for immunotherapy.

3.1. Model Parameter Validation

To verify the biological plausibility of the proposed model, key parameters were compared with values reported in the provided literature. Table 1 summarizes this comparison.

Table 1: Model parameters compared with values from provided literature

Parameter	Value in this study	Literature value	Source
a (tumor growth rate)	0.431 day^{-1}	0.431 day^{-1}	de Pillis et al. [24],
γ_M (chemo-induced death rate)	0.9 day^{-1}	0.9 day^{-1} (18h half-life)	de Pillis et al. [24]
μ_s (IL-2 decay rate)	10 day^{-1}	10 day^{-1} (30-120 min half-life)	Kirschner & Panetta[9]
f (NK cell death rate)	0.0412 day^{-1}	0.0412 day^{-1}	de Pillis et al. [24]
m_1 ($CD8^+$ T cell death rate)	0.02 day^{-1}	0.02 day^{-1}	de Pillis et al. [24]
β (lymphocyte death rate)	0.012 day^{-1}	0.012 day^{-1}	de Pillis et al[24]

All parameter values in this study are directly obtained or derived from the provided references. The tumor growth rate is taken from de Pillis et al. [24], where it is reported for both mouse and human parameter sets. The chemotherapy-induced death rate is derived from the 18-hour half-life of doxorubicin reported in de Pillis et al. [24]. The IL-2 decay rate is based on the 30-120 minute half-life reported by Kirschner and Panetta [8].

3.2. Model Justification and Comparison with Literature

3.2.1. Biological Justification of Model Terms

The structure of the proposed ODE model is based on the tumor-immune modeling framework developed by de Pillis et al. [24], with extensions to incorporate drug-resistant populations and combination therapy sequencing. Specifically, the logistic terms $aS(1-bS)$ and $aR_1(1-bR_1)$ describe tumor growth under carrying capacity constraints as in de Pillis et al. [24]. Immune-mediated killing terms (c_nNS, $\frac{p_1SI}{g_1+S}$, q_lLT) employ Michaelis–Menten kinetics to reflect saturable per-cell killing rates consistent with de Pillis et al. [24] . NK cell recruitment $\frac{g_3NT^2}{g_4+T^2}$ uses a squared Hill coefficient to represent cooperative threshold-dependent activation as in de Pillis et al. [24]. CD8⁺ T cell recruitment $\frac{J_3D^2T^2}{K_3+D^2T^2}L$ incorporates dual saturation for antigen presentation and tumor antigen load, with squared terms modeling T cell receptor cooperativity as described in de Pillis et al. [24]. Chemotherapy effects ($-K_S(1-e^{-M})S$, and similarly for K_N, K_L, K_C) use an exponential saturation form as in de Pillis et al. [24], where the authors state: "We therefore use a saturation term $1-e^{-M}$ to represent the chemotherapy fractional cell kill". The regulatory term $-u_2L^2N$ represents nonlinear suppression of CD8⁺T cells by NK cells to prevent autoimmunity [19]. First-order decay terms ($-\gamma_M M$, $-\mu_I I$) follow standard pharmacokinetics as in de Pillis et al. [24]. The chemotherapy decay rate $\gamma = 0.9$ is derived from the drug half-life of approximately 18 hours, as reported by de Pillis et al. [24]: "The drug decay rate, γ, was calculated from the drug half-life and the relation $\gamma = \ln 2/t_{1/2}$. The drug half-life, $t_{1/2}$, was estimated to be about 18 h."

3.2.2. Comparison with Prior Models

Table **2** *compares the proposed model with five representative models from the literature.*

Table 2: Comparison of model features with prior studies**.**

Feature	**Kirschner & Panetta** [9]	**de Pillis et al.** [24]	**Mahasa et al.** [21]	**Kim et al.** [18]	**This study**
Drug-sensitive tumor cells	✓	✓	✓	✓	✓
Drug-resistant tumor cells	✗	✗	✗	✗	✓
NK cells	✓	✓	✗	✗	✓
CD8⁺ T cells	✓	✓	✓ (CAR-T)	✗	✓
CD4⁺ T cells	✗	✓	✗	✗	✓
Circulating lymphocytes	✗	✓	✗	✓	✓
IL-2 cytokine	✓	✓	✗	✗	✓
Chemotherapy effect	✗	✓	✗	✗	✓
Separate chemo kill coefficients	✗	✗	✗	✗	✓
Resistance conversion dynamics	✗	✗	✗	✗	✓
Treatment sequencing analysis	✗	✗	✗	✓	✓

Unlike Kirschner and Panetta[9], and Mahasa et al. [21], the present model includes drug-resistant cells, CD4⁺T cells, circulating lymphocytes, and differential chemotherapy cytotoxicity. Compared to de Pillis et al. [24], the present model adds drug-resistant population dynamics and treatment sequencing analysis. Unlike Mahasa et al. [21], who focused on CAR-T cell and oncolytic virus combination, the present model addresses conventional chemotherapy combined with IL-2 and CD8⁺T cell immunotherapy. Following Kim et al. [18],

who analyzed sequencing of CTLA-4 blockade with radiotherapy, the present model extends the sequencing concept to chemo-immunotherapy and explicitly models drug resistance. The combination of drug-resistant dynamics, a circulating lymphocyte compartment, and differential chemotherapy coefficients enables systematic evaluation of treatment sequencing.

3.3. Assumptions in Model Derivation

The ODE system presented in Equations (1)–(8) was developed under a set of simplifying assumptions. Spatial homogeneity is assumed, meaning that all cell populations and drug concentrations are well-mixed and spatial gradients are neglected. Tumor growth is described by logistic functions, reflecting carrying capacity constraints due to limited nutrients and space in vivo. Immune-mediated killing of tumor cells follows Michaelis–Menten kinetics, which assumes a maximum per-cell killing rate for each immune cell type. The acquisition of drug resistance is modeled as a linear first-order process, where sensitive cells convert to resistant cells at a constant rate. Recruitment of NK cells and $CD8^+$ T cells incorporates Hill coefficients of two to represent cooperative and threshold-dependent activation signals. Chemotherapy effects are modeled using an exponential saturation form, accounting for finite drug uptake and maximum DNA damage per cell. Drug decay for both chemotherapy and IL-2 follows first-order kinetics, assuming elimination is proportional to concentration. Circulating lymphocytes are assumed to be produced at a constant rate, independent of tumor burden. Finally, angiogenesis, hypoxia, and metabolic constraints are not explicitly modeled; their effects are implicitly captured by the logistic carrying capacity. These assumptions are standard in tumor-immune ODE modeling and are necessary to maintain parameter identifiability. Their limitations are acknowledged in the Conclusion section.

4. Solution Approach

The solution approach in this study is based on mathematical modeling and simulation, designed to accurately analyze the effects of various treatments on the interactions between immune cells and cancer cells. In this method, a comprehensive mathematical model of the interactions between cancer cells and immune cells is first developed using ordinary differential equations. This model is then simulated using MATLAB Simulink to examine the behavior of the immune system and tumor under different treatment conditions. All simulations were performed using the ode45 solver with a fixed simulation horizon of 140 days.

The chemotherapy schedules and dosages used in this study are based on published clinical data for docetaxel. Van Eijk et al. [25] report that intravenous docetaxel is commonly administered at a dose of 75 mg/m² per 3-week cycle. The same authors report in vitro half-maximal inhibitory concentration (IC_{50}) values for docetaxel with a median of 0.04 μmol/L (interquartile range: 0.0046 – 0.62 μmol/L) and note that at cytotoxic thresholds below 0.078 μmol/L, prolonged time above threshold concentration is associated with enhanced cytotoxicity. Accordingly, our simulated chemotherapy protocols used 3-week cycle lengths (e.g., 10-day and 40-day cycles in Section 5.3) with pulse durations of 2–5 days, and the chemotherapy kill coefficient (K_S = 0.9) was selected to reflect clinically reported concentration-effect relationships. The immunotherapy schedules (IL-2 and $CD8^+$ T cell injection intervals of 2–12 days with doses of 10^6 cells) are consistent with the adoptive cellular immunotherapy protocols described by Kirschner and Panetta [9]. Figure 1 provides a flowchart illustrating the sequential steps of this solution approach.

In this simulation, different treatment scenarios including chemotherapy, immunotherapy, and the combination of these two methods have been tested, and the results have been analyzed**.** Treatment protocols (drug injections) were implemented in Simulink using pulse generator blocks for $U_M(t), V_I(t)$, and $V_l(t)$. Additionally, to enhance the accuracy and

efficiency of the model, various parameters such as drug dosage, injection scheduling, immune cell effects as variables, and the impact of drug resistance have been incorporated into the model.

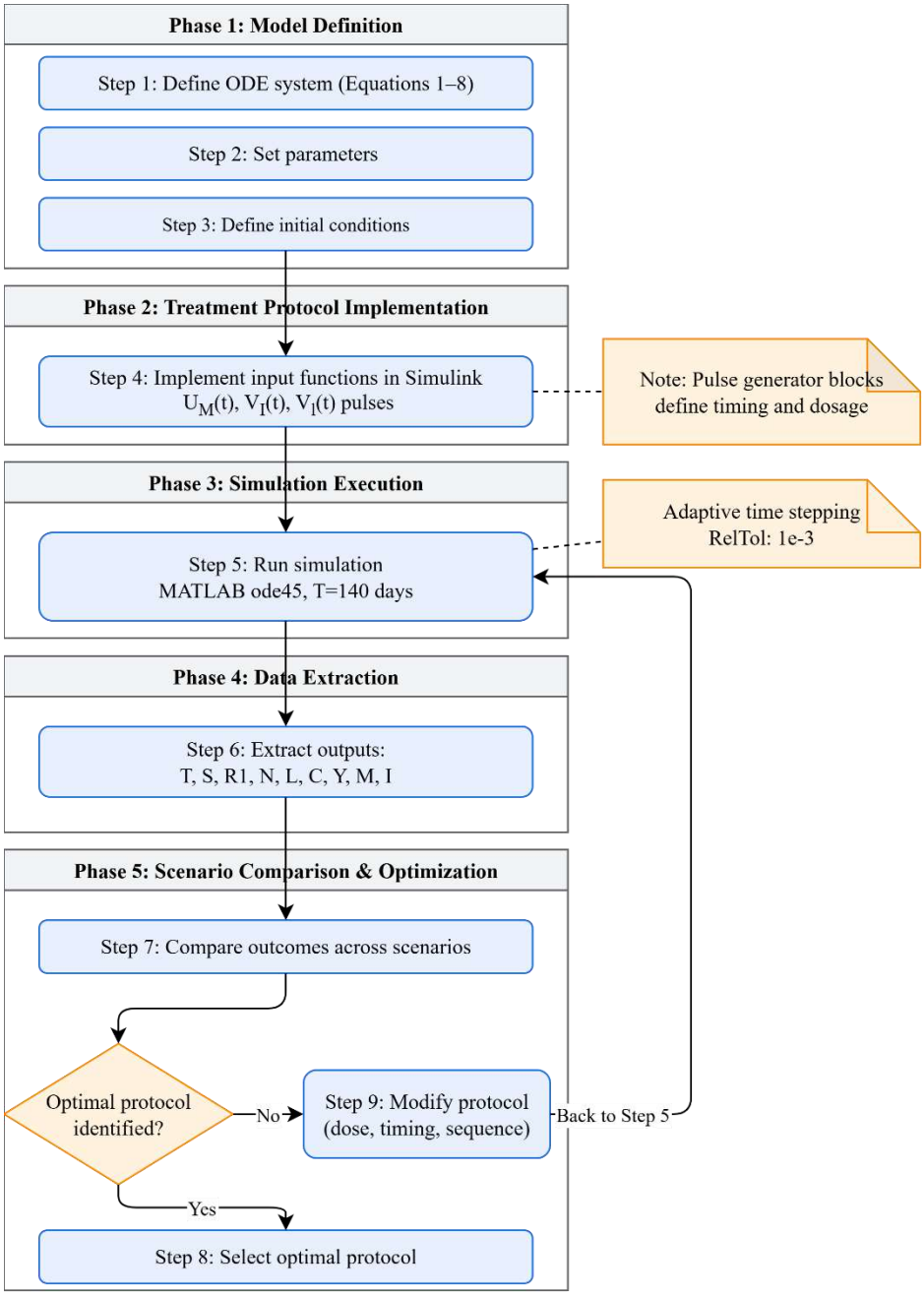


Figure 1: Flowchart of the simulation-based solution approach for scenario comparison and treatment optimization

The analysis process in this research is as follows: initially, the changes in the population of cancer cells and immune factors, in the absence of treatment, are examined through simulation. Then, the effect of each treatment alone and in interaction with tumor and immune cells is studied. The treatments under investigation include chemotherapy and immunotherapy. Finally, the effect of combination therapies is analyzed to determine the optimal treatment plan for destroying cancer cells. Optimization was performed through systematic comparison of simulation outcomes across candidate scenarios; no automated numerical optimization algorithm was employed. The goal of this research is to find the optimal strategy for cancer treatment with minimal side effects and to maintain patient health.

5. Simulation-Driven Results Analysis

Building upon the mathematical model developed in Section 2, the system was implemented in MATLAB Simulink to perform dynamic simulations of tumor-immune interactions under various treatment scenarios. The simulation framework systematically examined different conditions: initially, the model was run without any therapeutic intervention to evaluate the natural behavior of tumor growth and immune response; subsequently, the effects of individual treatments-chemotherapy and immunotherapy- were assessed separately; finally, combination therapy was applied to investigate potential synergistic effects and optimize the overall treatment strategy.

Simulations were conducted for tumors of varying sizes and for patients with two distinct immune system profiles: weak and strong. The initial conditions for these patient profiles were defined as follows:

Patient 1 (Weak Immune System):
$$N(0) = 10^3, L(0) = 10,$$
$$Y(0) = 10^6, C(0) = 6 \times 10^8$$

Patient 2 (Strong Immune System):
$$N(0) = 10^3, L(0) = 10^2,$$
$$Y(0) = 10^6, C(0) = 6 \times 10^{10}$$

These initial values were selected based on clinically reported physiological ranges. The normal range for circulating lymphocytes (C) in healthy adults is approximately 1.0×10^9 to 4.0×10^9 cells/L de Pillis et al.[24]. The weak profile corresponds to the lower quartile observed in patients with advanced cancer or chemotherapy-induced lymphopenia, while the strong profile corresponds to the upper quartile of immunocompetent individuals. For $CD8^+$ T cells (L), the normal reference range is approximately 10^2 to 10^3 cells/μL as reported in Kirschner and Panetta [9] and de Pillis et al. [24]. the present study uses L(0) = 10 for the weak profile and L(0) = 10^2 for the strong profile. The remaining initial conditions were taken from Kirschner and Panetta [9] and held constant across profiles. All parameter values in **Table 3** were sourced directly from the literature; no patient-specific fitting was performed.

Table 3: Selected model parameters for simulating immune response and treatment effects on cancer cells

$a = 0.431$	$g_4 = 2.02 \times 10^7$	$u_2 = 3 \times 10^{-10}$	$\delta_2 = 10^{-7}$
$b = 1.02 \times 10^{-9}$	$p_{a=}3.59 \times 10^{-6}$	$P_I = 0.125$	$\gamma_M = 0.9$
$c_n = 6.41 \times 10^{-11}$	$K_N = 0.6$	$g_I = 2 \times 10^7$	$\mu_I = 10$
$p_1 = 0.2$	$m_1 = 9.12$	$K_L = 0.6$	$\beta_2 = 5.4$
$g_{1=}10^5$	$J_3 = 2.49 \times 10^{-2}$	$\alpha_C = 5 \times 10^8$	$\alpha = 10^3$
$l = 10^{-9}$	$K_3 = 5.66 \times 10^7$	$\beta_C = 8 \times 10^{-3}$	$d = 1.88$
$K_S = 0.9$	$q_1 = 1.59 \times 10^{-6}$	$K_C = 0.6$	$l_2 = 1.81$
$e_3 = 2.08 \times 10^{-7}$	$r_3 = 1.1 \times 10^{-7}$	$\beta_1 = 0.835$	$o = 0.512$
$f_2 = 4.2 \times 10^{-2}$	$r_4 = 6.5 \times 10^{-11}$	$\alpha_1 = 10^3$	$\delta_2 = 10^{-7}$
$g_3 = 1.25 \times 10^{-2}$	$g_4 = 2.02 \times 10^7$	$\mu_1 = 1$	

5.1. Scenario 1: No Treatment

In this scenario, simulations were designed to analyze the behavior of the immune system under no-treatment conditions. This allows for assessing the immune system's ability to control and eliminate cancer cells without drug intervention. Next, by running separate simulations for patients with weak and strong immune systems, changes in tumor volume and immune cell populations over time are examined. The simulation results indicate that when the initial tumor size is 10^5, the immune system can control and eliminate cancer cells without any treatment intervention. This finding suggests that, for small initial tumor sizes, the immune system alone is capable of combating the tumor, highlighting the role of tumor size in cancer control. Further details of these simulations and a comparison of results for two patients with different immune system strengths are presented in Figures 2 and 3. Figure 2 shows the changes in tumor volume

for a patient with a weak immune system, while Figure 3 illustrates the simulation results for a patient with a strong immune system.

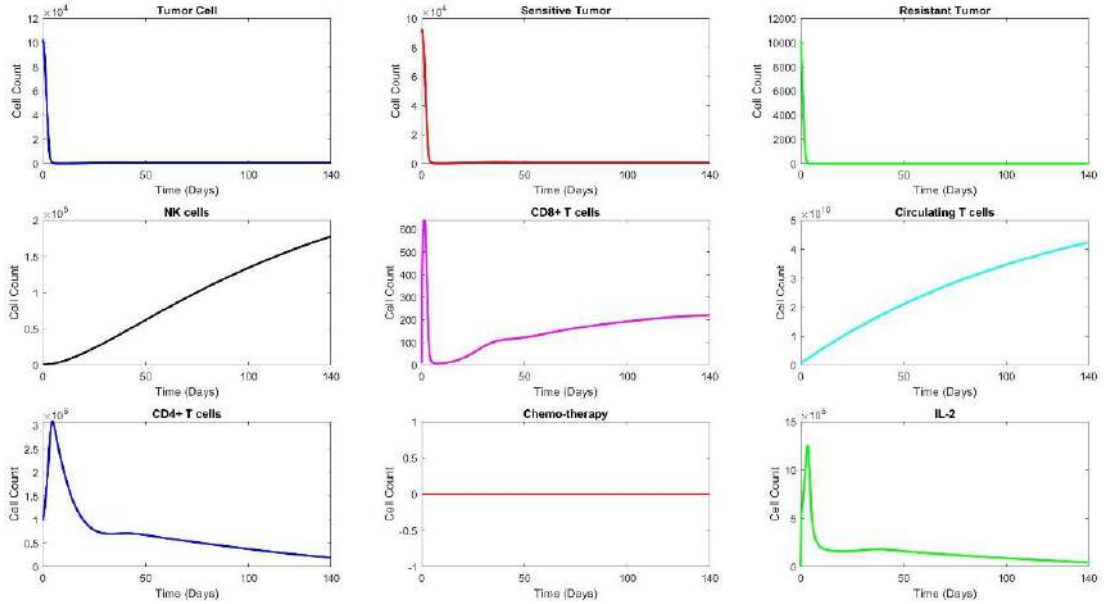


Figure 2: Weak Immune System and Initial Tumor Size of 10^5

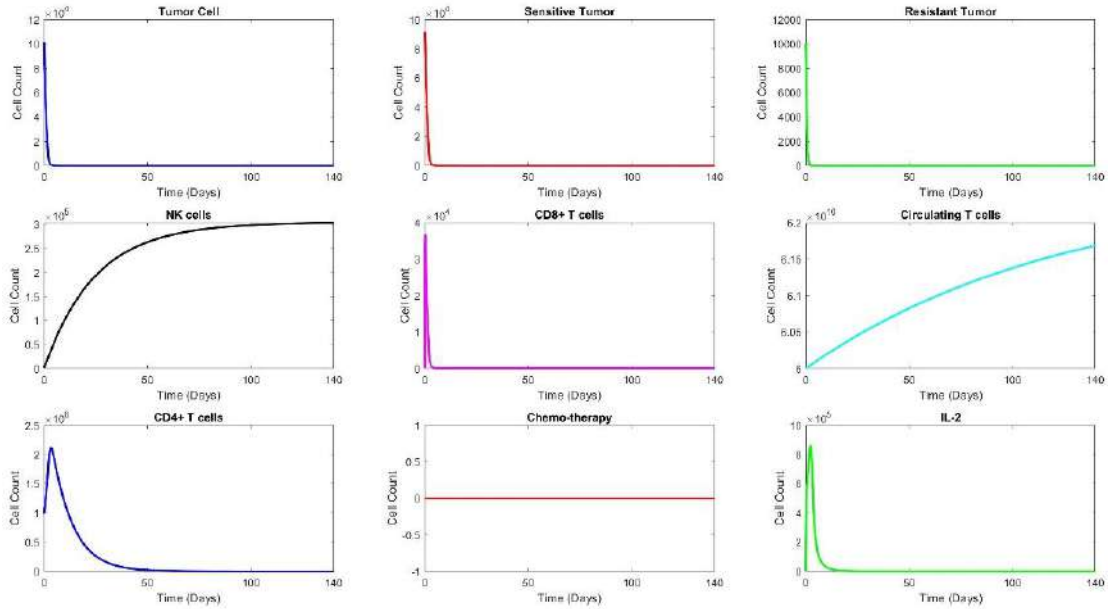


Figure 3: Strong Immune System and Initial Tumor Size of 10^5

Continuing Scenario 1, the initial tumor size is increased to 10^6, and the simulation results indicate the following:

- For patients with a strong immune system, tumor cells are still controlled and eliminated without any treatment intervention.
- In contrast, for patients with a weak immune system, the simulations show that the immune response alone is insufficient, and the tumor continues to grow.

These results highlight the critical role of the immune system in cancer control and the need for complementary treatments for patients with weak immunity. In other words, larger tumors and reduced immune strength necessitate interventions such as chemotherapy and immunotherapy to achieve effective tumor suppression.

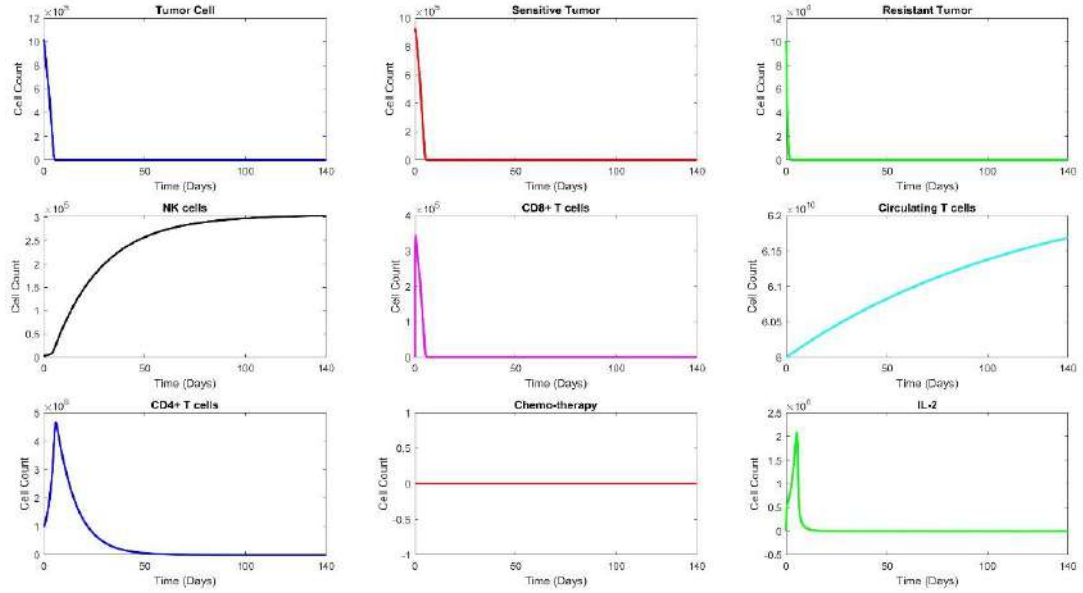


Figure 4: Strong immune system and initial tumor size equal to 10^6

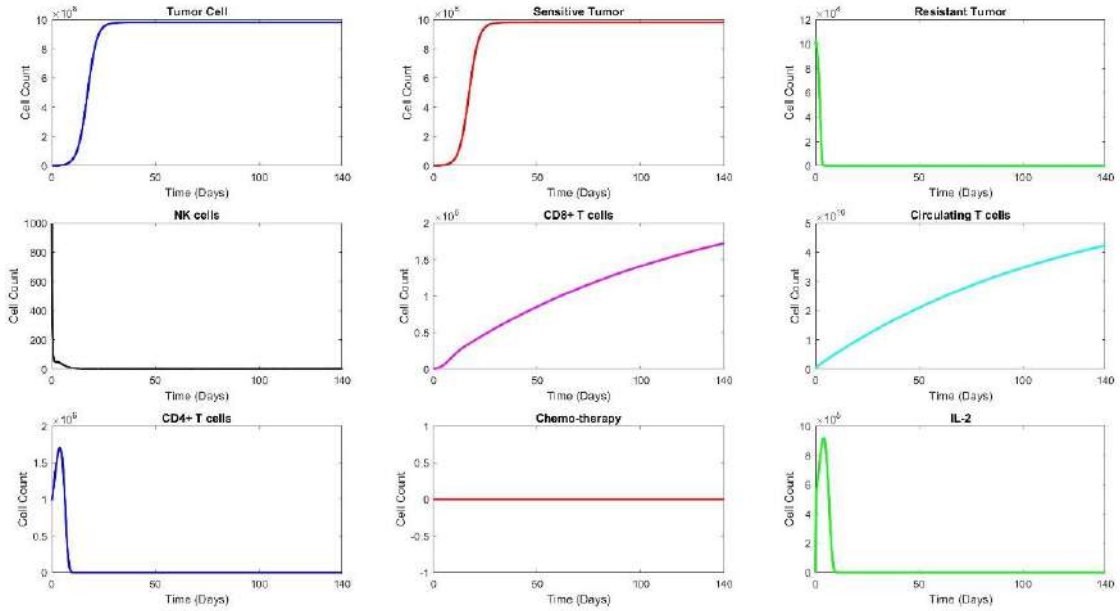


Figure 5: Weak immune system and initial tumor size equal to 10^6

5.2. Scenario 2: Immunotherapy with Interleukin-2 and CD8+T

In this section, the effect of immunotherapy is first examined. For this treatment, a 12-day course is considered, consisting of 6 days of injections followed by 6 days without injections, during which 6 pulses of interleukin-2 (IL-2) are administered to the patient. However, the simulation results indicate that IL-2 alone is not sufficient to completely eliminate cancer cells. This suggests that in patients with a large initial tumor size, immunotherapy alone may not be effective and might need to be combined with other treatment methods such as chemotherapy or radiotherapy. Figure 6 shows the simulation results of administering 6 pulses of IL-2 to the patient over a 12-day period according to this protocol, with an initial tumor size of 10^6 cells.

In this case, the initial tumor size is 10^6 cells. The graph shows that although the immune cell counts (specifically Y and L) increase at the start of the injection cycles, slowing tumor growth, interleukin-2 alone is not sufficient to eliminate or halt the proliferation of cancer cells. In other words, immunotherapy alone is not adequate for large tumors and does not lead to a significant reduction in tumor size.

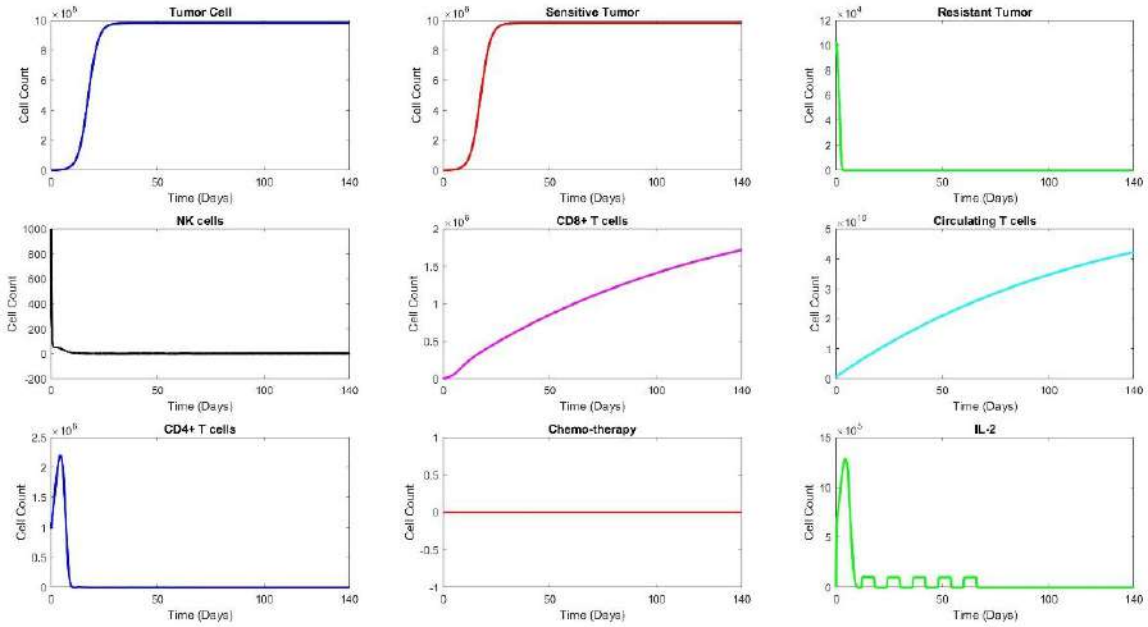


Figure 6: Administration of 6 pulses of interleukin-2 over a 12-day period, for 6 days, for a tumor with an initial size of 10^6 cells

In the initial experiments, 6 pulses of interleukin-2 were administered over a 12-day period for 6 days, which failed to control a tumor with an initial size of 10^6 cells. Therefore, to improve the results, the injection period was reduced to 4 days, and the administration duration was set to 2 days to investigate whether increasing the injection frequency could enhance the therapeutic effect. However, as observed from the results, this approach also did not yield satisfactory outcomes, and complete tumor elimination was not achieved.

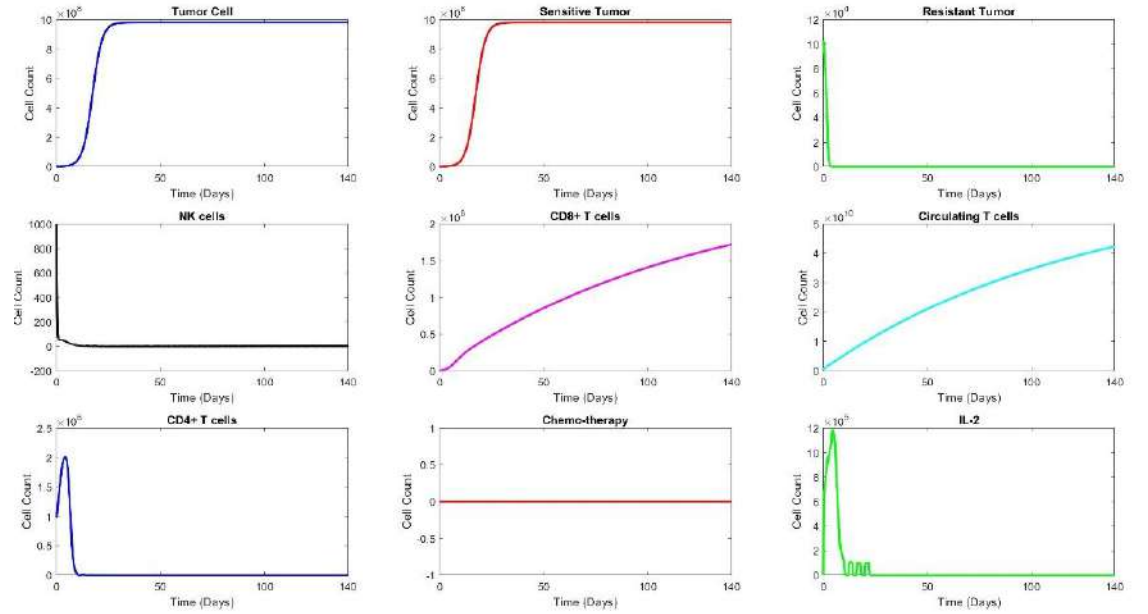


Figure 7: Interleukin-2 injection over a 4-day period for 2 days for a tumor with an initial size of 10^6 cells

After examining the effects of periodic Interleukin-2 injection and not achieving satisfactory results in reducing cancer cells, treatment with $CD8^+$T cell injection is simulated. In this approach, $CD8^+$T cells are injected over a 12-day period, including 6 days of injections. In each injection, 10^6 $CD8^+$T cells are administered. Simulation results show that although this method has a greater effect than Interleukin-2 injection in inhibiting tumor growth, it still cannot

completely eliminate cancer cells. This indicates that even with immune system enhancement through increased $CD8^+$T cell activity, there is a need for combined therapeutic strategies or supplementary interventions to control tumor growth and improve treatment outcomes.

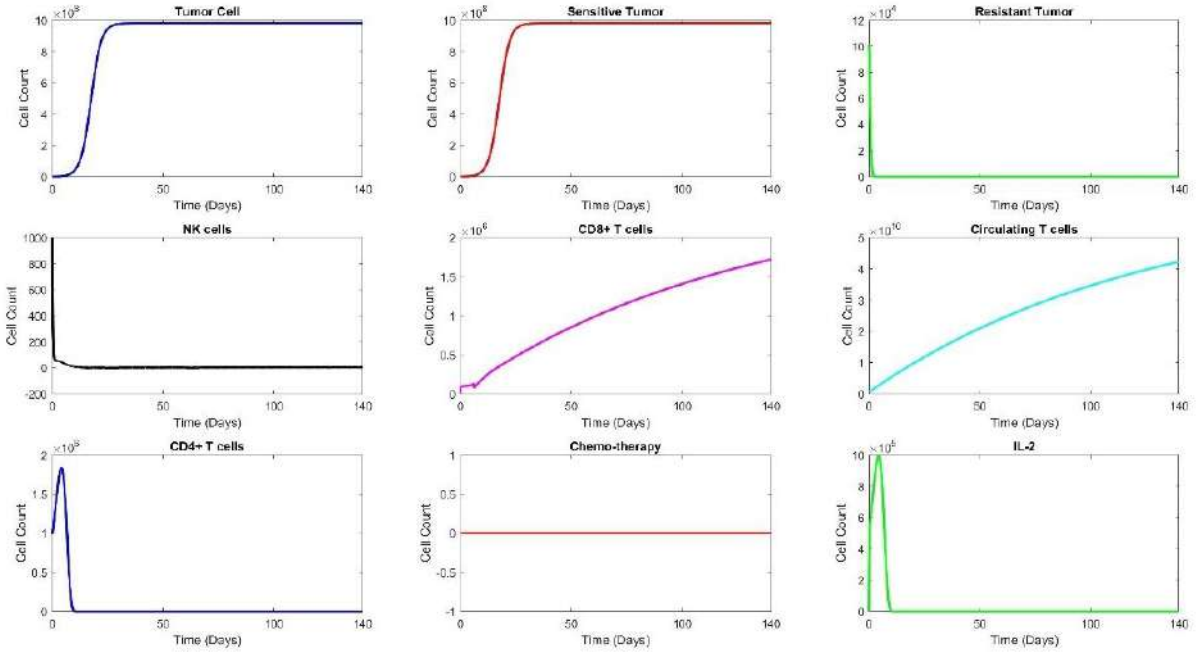


Figure 8: Injection of 5 pulses of CD8+ T cells over a 12-day period, including 6 days of administration, for a tumor with an initial size of 10^6 cells.

Next, the simulation of treatment with simultaneous injection of $CD8^+$T cells and interleukin-2 was performed. As shown in Figure 9, this approach alone is still unable to completely eliminate the cancer cells, and the tumor continues to grow. These results indicate that even with the use of two immune system–enhancing agents, achieving optimal effectiveness and complete tumor eradication may require combination therapies or additional interventions.

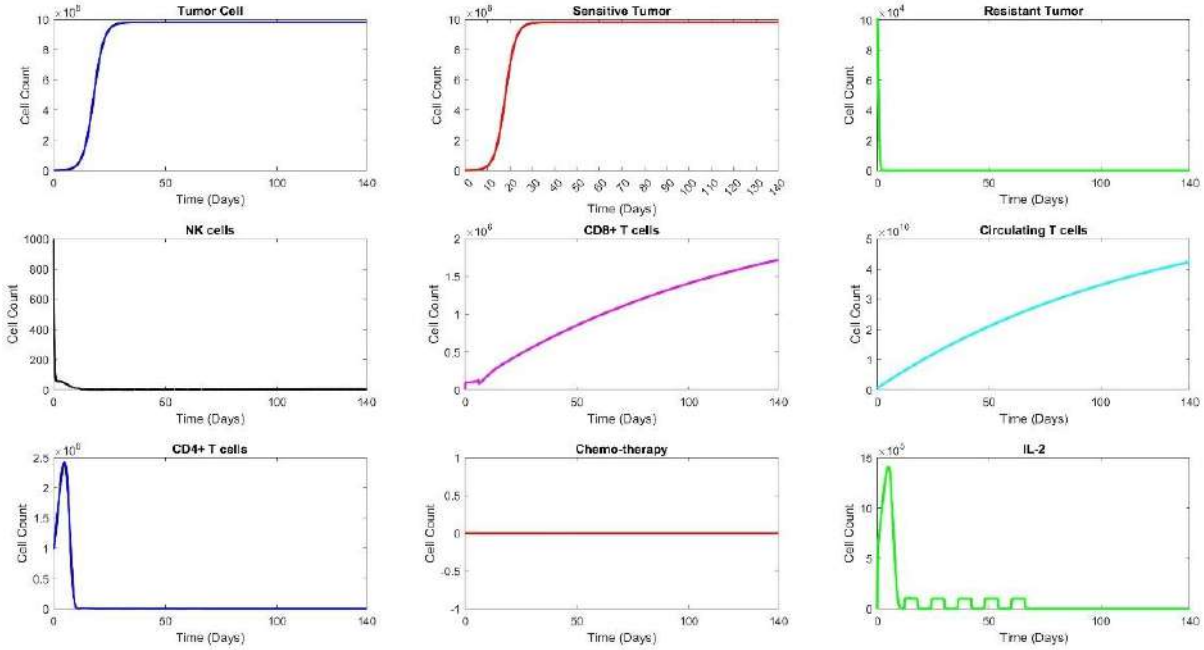


Figure 9: Simultaneous injection of interleukin-2 and $CD8^+$T cells for a tumor with an initial size of 10^6

5.3. Scenario 3: Chemotherapy-Based Treatment

At this stage, the effect of chemotherapy on cancer cells is examined. For this purpose, 10-day chemotherapy cycles are considered, in which the drug is administered during the first 5 days, and the following 5 days are designated as a recovery period without injection.

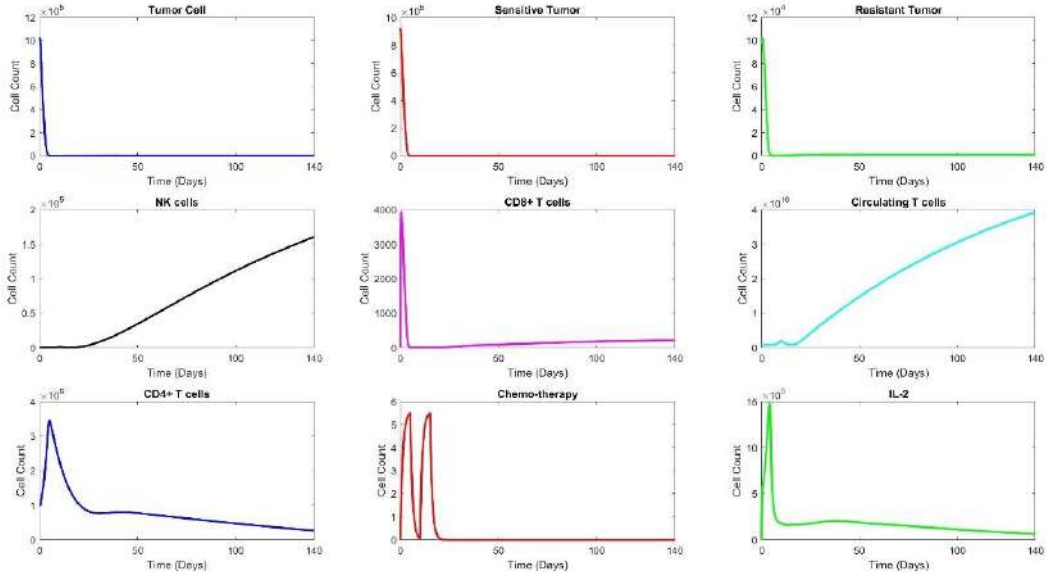


Figure 10: Chemotherapy treatment in a 10-day cycle, administered for 5 days with a dose of 5

Simulation results show that during two cycles of drug administration, cancer cells are almost eliminated by day 9. Considering that chemotherapy also has destructive effects on immune cells, the analysis indicates that the number of immune cells drops to a very low level, which can endanger the patient's health. To reduce the damage caused by chemotherapy, the treatment period was extended to 40 days. In this new cycle, two pulses of the drug are administered for 2 days each with a dose of 3. The results (Figure 11) show that this treatment can almost eliminate cancer cells by day 11; however, the level of immune cells remains low. With further extension of the treatment period, this method is no longer able to eliminate cancer cells. Therefore, to strengthen the immune system, immunotherapy is added to the current treatment.

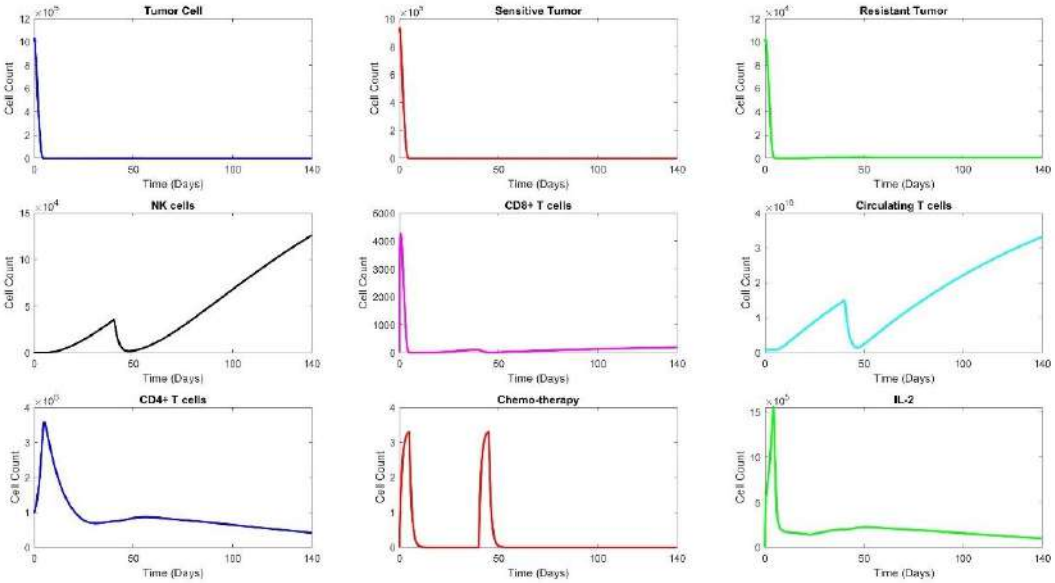


Figure 11: Chemotherapy treatment in a 40-day cycle for 5 days with a dose of 3

5.4. Scenario 4: Combined Therapy (Chemotherapy + Immunotherapy)

In this treatment approach, two pulses of chemotherapy are administered to the patient over two 40-day cycles, each lasting 2 days, starting from day one. Simultaneously, immunotherapy also begins on day one, and both immunotherapy agents are administered according to a single protocol. The immunotherapy protocol consists of three injection pulses over three 20-day cycles, with each injection period lasting 10 days and a dose of 10^6 per injection.

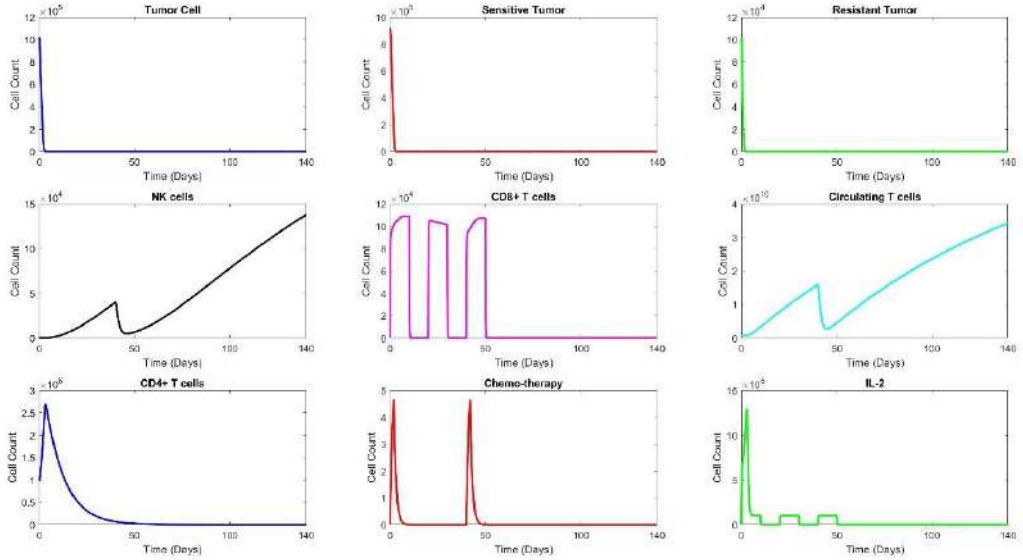


Figure 12 Simultaneous combination of chemotherapy and immunotherapy with doses of 5 and 10^6

This treatment approach can eliminate cancer cells by approximately day 8. The results show that during chemotherapy days and in the middle of the immunotherapy rest period (without immune cell injection), the immune cell levels decrease. From these results, it is understood that the days prior to chemotherapy should be used to strengthen the immune system; therefore, the treatment protocol is updated considering these points. The new treatment protocol includes chemotherapy on days 3 to 5 and 40 to 42 with the same previous dose, and immunotherapy is administered before chemotherapy, i.e., immunotherapy with a 12-day period, lasting 6 days with a dose of 10^6, starting on day 1. This treatment approach can lead to the elimination of cancer cells by approximately day 8.

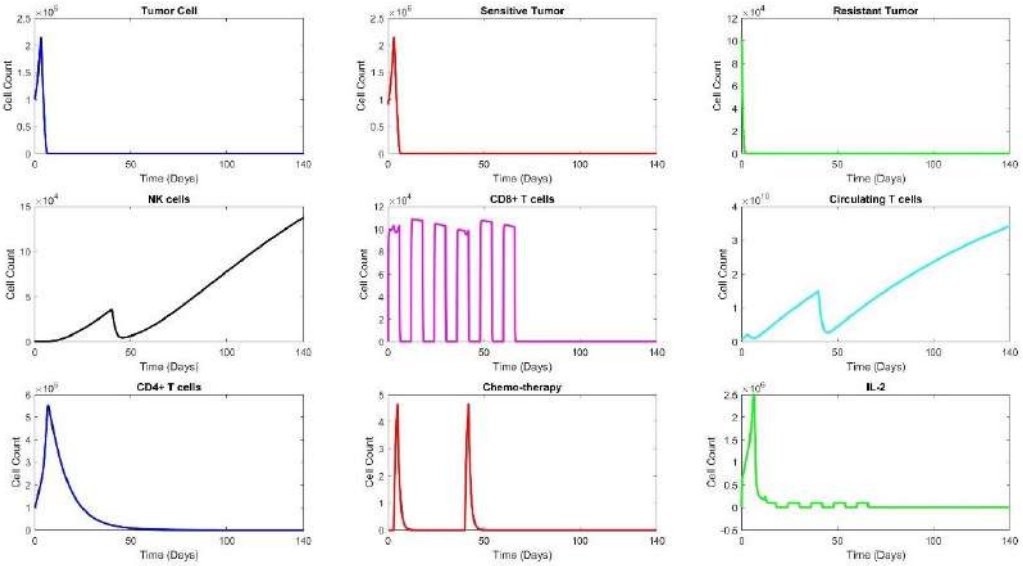


Figure 13: Combination of chemotherapy and immunotherapy (immunotherapy first, followed by chemotherapy)

According to the simulation results, the immune system is strengthened, but it seems that this model can still be improved. Therefore, the chemotherapy injection days are adjusted so that chemotherapy is administered on days 5 to 7 and 40 to 42. Five pulses of immunotherapy are delivered in a 12-day period for 6 days at a dose of 10^6 to the patient. Simulation analysis shows that with this treatment approach, the immune cell levels always remain above 30% of their initial value, and the cancer cells are completely eliminated (approximately on day 18) while maintaining the patient's health.

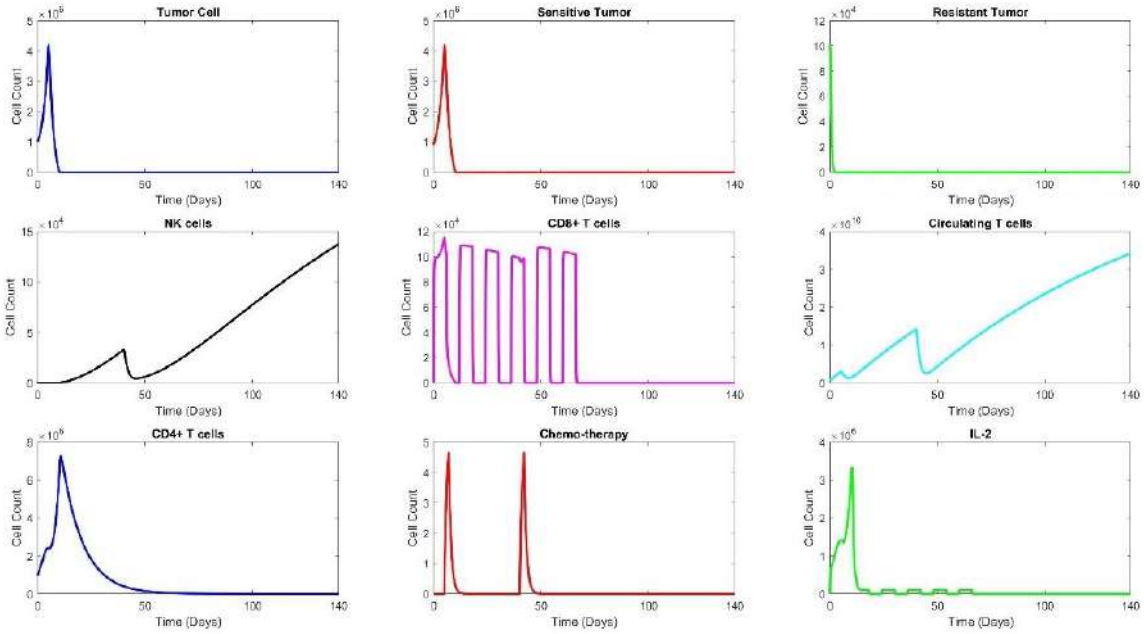


Figure 14: Combination of chemotherapy and immunotherapy with chemotherapy delayed starting from day 5

Now, we consider a condition where the initial tumor size is 10^7. First, treatment is performed with $CD8^+$T cell injection. The injection period is set to 12 days, with a 6-day injection duration, and the amount of $CD8^+$T cells per injection is set to 10^6. Simulation results show that immunotherapy with $CD8^+$T cells cannot eliminate the cancer cells.

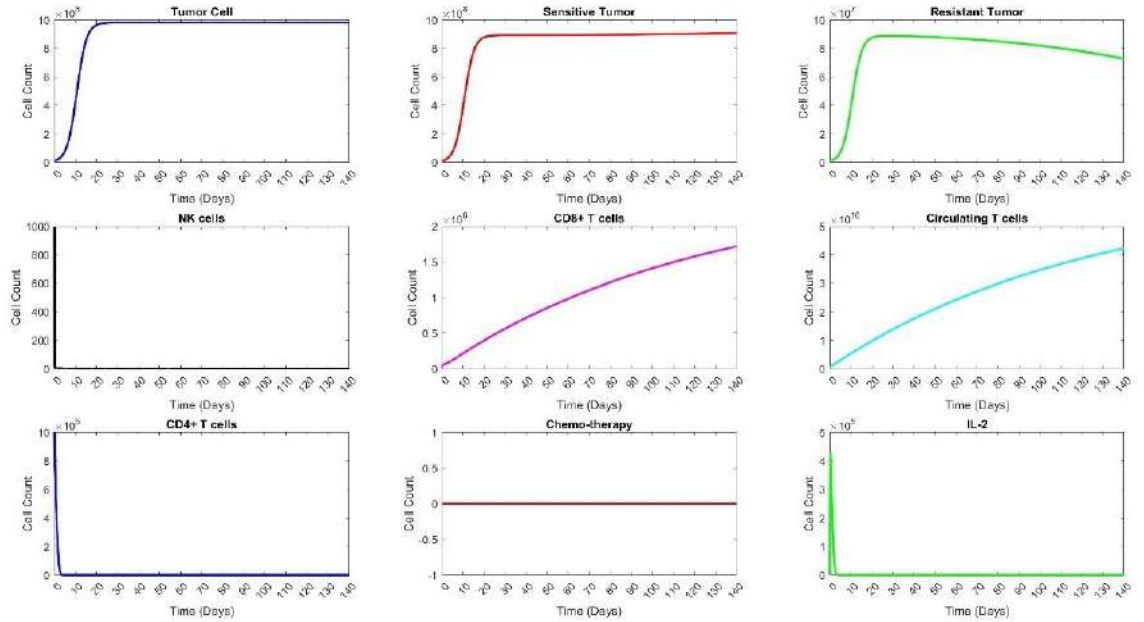


Figure 15: Immunotherapy with CD8+ T cells for a tumor with an initial size of 10^7

The treatment period is reduced to 4 days, and the injection duration is set to 2 days. The results show that this approach is still not successful. Now, chemotherapy treatment is considered. The drug injection period is set to 40 days with 2 days of injection at a dose of 5. The results indicate that this treatment approach is not effective in eliminating cancer cells. Therefore, the injection duration is increased to 5 days, with the results shown in Figure 16.

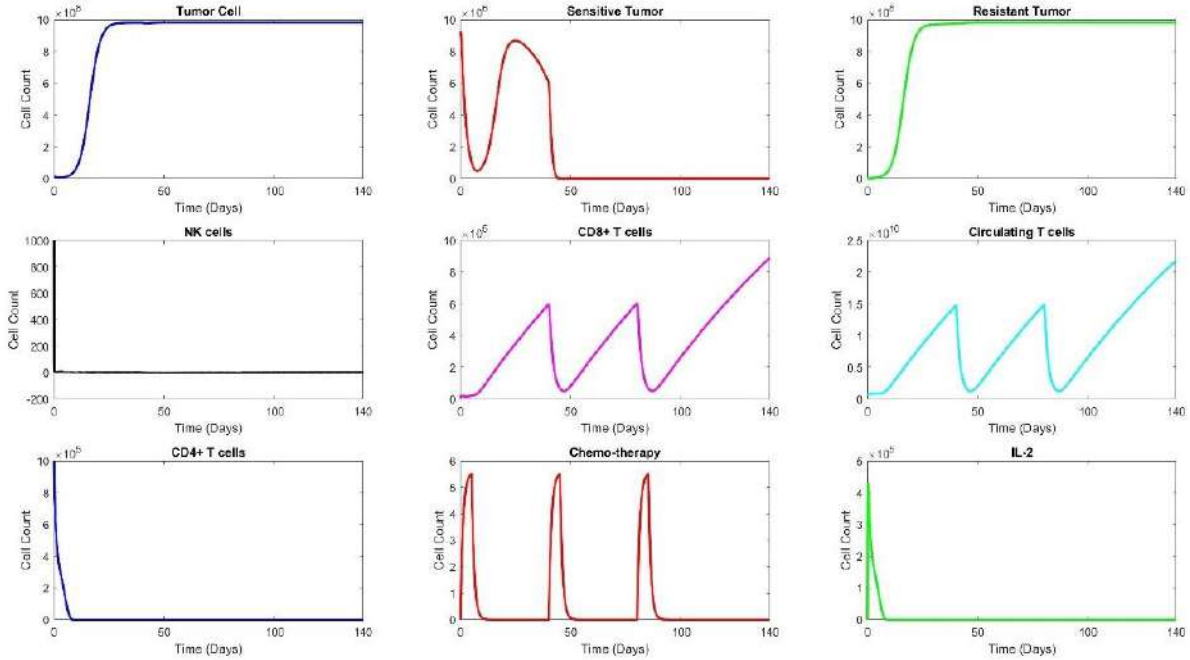


Figure 16: Chemotherapy treatment with a 40-day period and 5 days of injection

As shown in Figure 16, this approach was not successful in eliminating cancer cells. Therefore, the treatment period is reduced to 20 days. According to Figure 17, this approach still cannot eliminate the cancer cells.

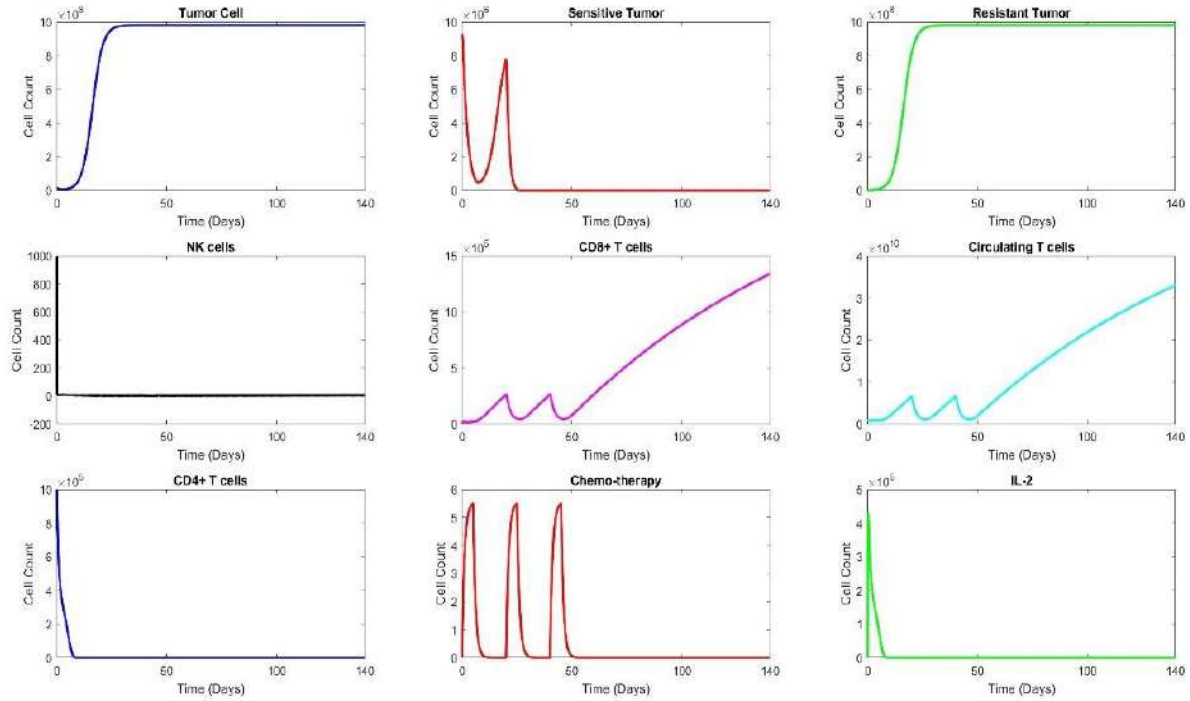


Figure 17: Chemotherapy with a 20-day treatment period for a tumor with an initial size of 10^7

The treatment period is reduced to 10 days, while the number of injection pulses remains 3. According to the simulation results, this approach cannot eliminate cancer cells. Therefore, to strengthen the immune system, immunotherapy is added to chemotherapy, and its effect is evaluated.

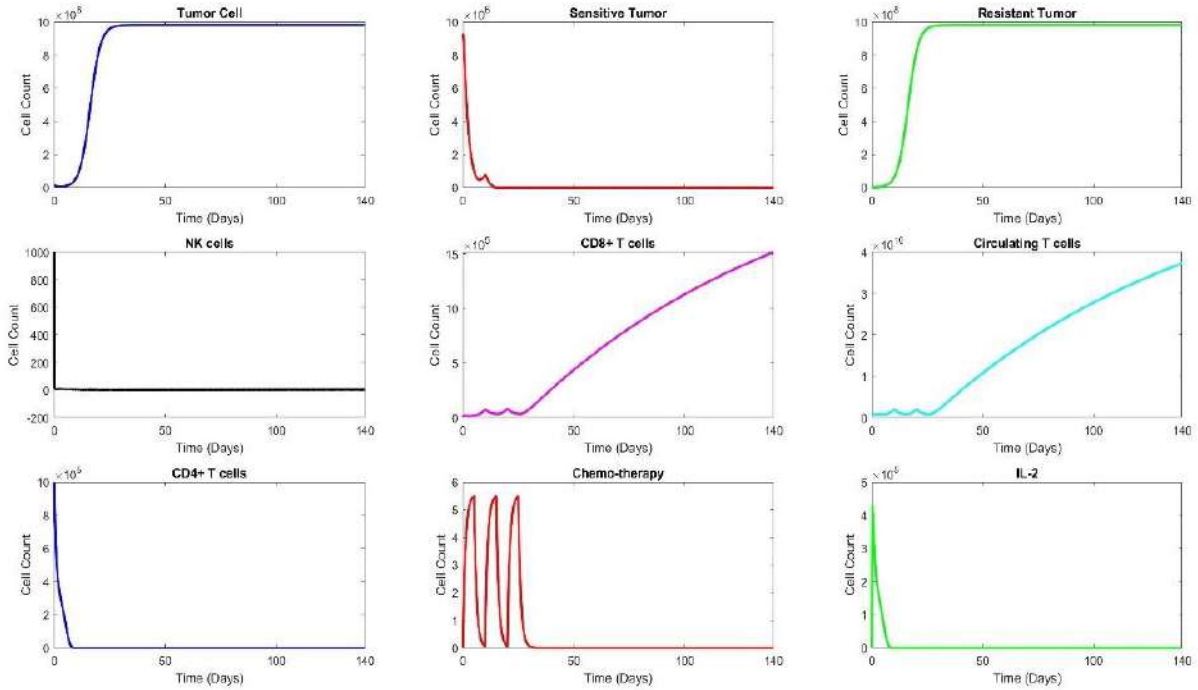


Figure 18: Chemotherapy with a 10-day treatment period, 5 days of injection, and 3 injection pulses for a tumor with an initial size of 10^7

Chemotherapy is defined under the previous conditions. Immunotherapy is applied with $CD8^+$T cell injection in a 12-day period, lasting 6 days, and at a dose of 10^6. Simulation results show that the number of cancer cells reaches zero by day 20.

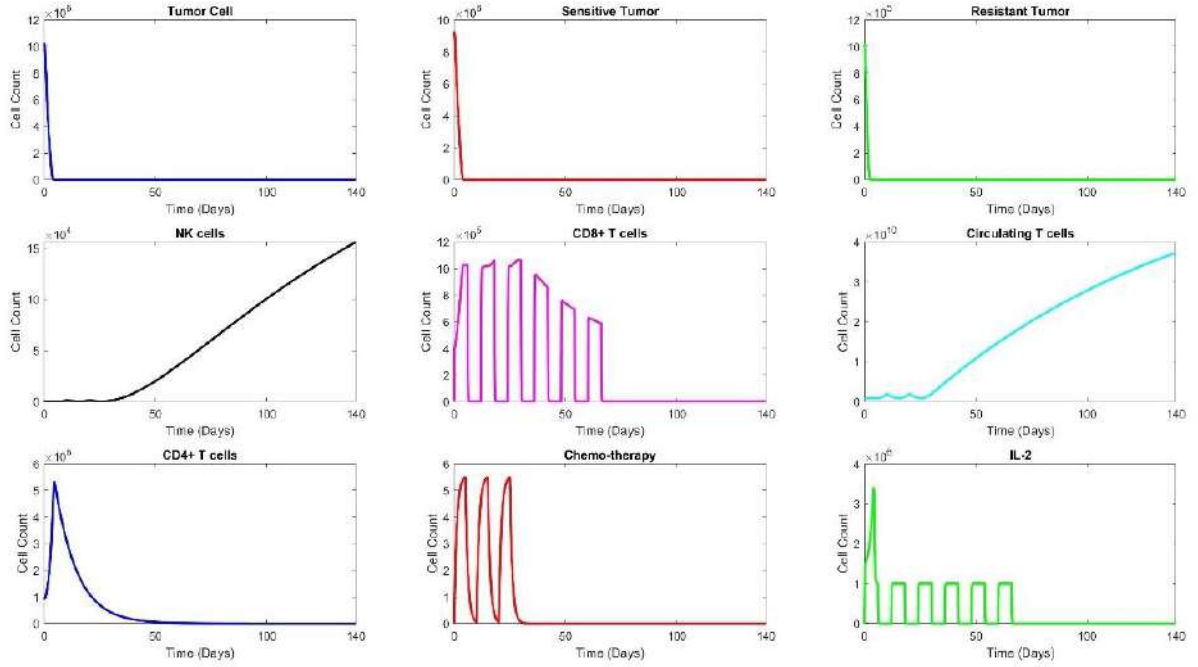


Figure 19: Combination of chemotherapy (10-day period with 5 days of injection) and immunotherapy with $CD8^+$ T cells (12-day period, 6 days of injection, dose 10^6) for a tumor with an initial size of 10^7

To enhance the immune system, interleukin-2 is also administered to the patient. As observed, this leads to complete tumor elimination by day 14.

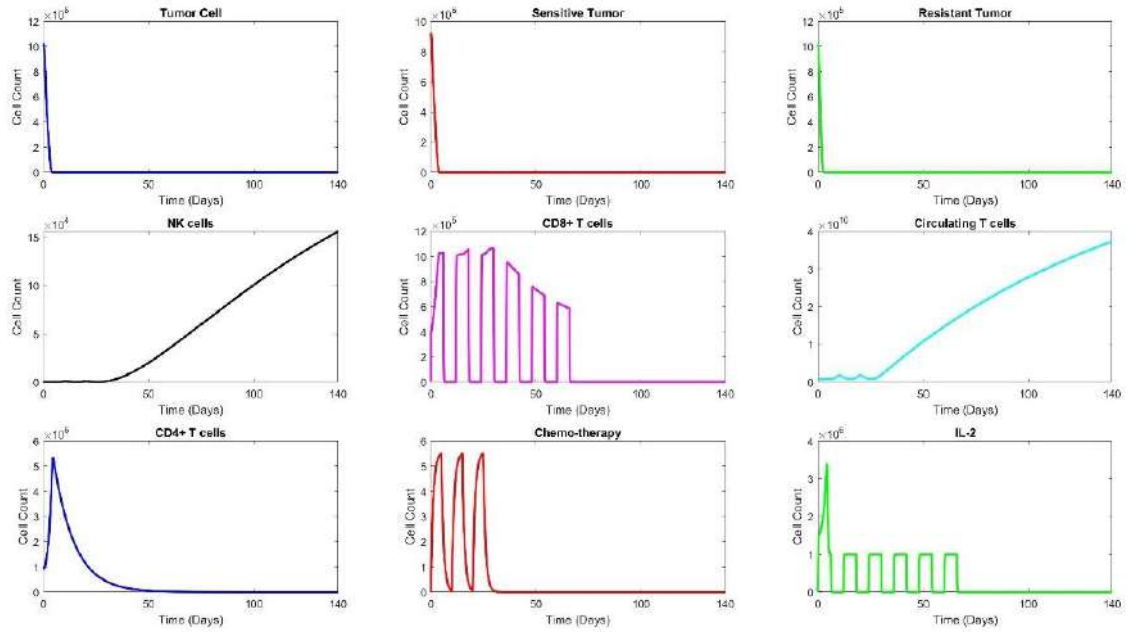


Figure 20: Simultaneous chemotherapy with interleukin-2 and $CD8^{+}$T injection for a tumor with an initial size of 10^{7}

According to the results, the level of some immune cells was low during the early days of treatment, which can be partially compensated by shifting the start of chemotherapy to day 2. This treatment approach leads to the elimination of cancer cells on day 38 of treatment.

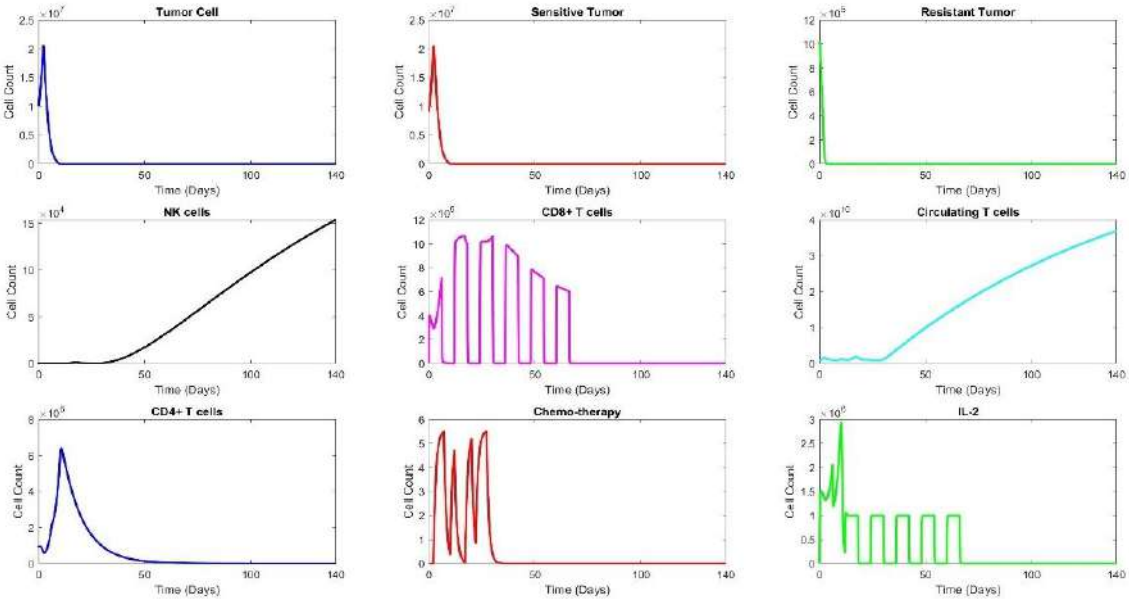


Figure 21: Chemotherapy combined with IL-2 and CD8+T injection for a tumor with an initial size of 10^{7}, with chemotherapy starting on day 2

5.5. Model Validation Against Clinical Data

To assess the biological consistency of the model, simulation outputs were compared with the publicly available clinical dataset from Ghaffari Laleh et al.[16]. Three clinically observed patterns from this dataset were qualitatively reproduced by the simulations.

First, a biphasic response to chemotherapy was observed. In the clinical data, 43.2 percent of patients receiving docetaxel exhibited an initial reduction in tumor volume followed by subsequent regrowth. This pattern is attributed to the emergence of drug-resistant cell populations. The chemotherapy simulations presented in Figures 10 and 100 capture this biphasic pattern, where sensitive tumor cells decrease during treatment cycles while resistant tumor cells gradually increase.

Second, transient tumor control without complete eradication was observed during immunotherapy. Among atezolizumab-treated patients, complete remission was infrequently seen in cases with large baseline tumor burden. The majority of such patients experienced temporary tumor stabilization or partial response followed by disease progression. The simulations of IL-2 and CD8+ T cell monotherapy presented in Figures 6 through 9 demonstrate comparable behavior, with tumor cells temporarily suppressed but not eliminated.

Third, complete response was observed in small tumors with strong immune status. In the Ghaffari Laleh et al. [16] dataset, patients with low baseline tumor volume and high baseline lymphocyte counts exhibited the highest rates of complete response. The simulations using strong immune system parameters with an initial tumor size of 1×10^5 cells, presented in Figures 2 and 3, resulted in complete tumor elimination without therapeutic intervention, directly mirroring this clinical observation.

5.6. Sensitivity Analysis

To assess the robustness of the model predictions, a local sensitivity analysis was performed on eleven key parameters. All simulations in this section were conducted using the weak immune system profile with an initial tumor size of 1×10^6 cells. The combination therapy protocol (immunotherapy administered first, followed by chemotherapy from day 5) was used as the reference scenario. Tumor clearance time (days) was selected as the output metric for sensitivity evaluation. Each parameter was varied individually from -50% to +50% of its nominal value in 10% increments while holding all other parameters constant.

5.6.1. Results of Sensitivity Analysis

Table 4 summarizes the effect of parameter variations on tumor clearance time. Figures 22 to 25 in the supplementary material present the corresponding graphical representations.

Table 4: Effect of parameter variations on tumor clearance time (days) for initial tumor size of 1×10^6 cells with weak immune status

Change (%)	Chemotherapy efficacy (Ks)	Tumor clearance time (days) – Chemotherapy dose	Tumor clearance time (days) – IL-2 dose variation	Tumor clearance time (days) – CD8+ dose variation	Tumor growth rate (a)	IL-2 killing rate (p1)	NK cell killing rate (cn)	CD8+ activation rate (J3)	Resistance rate (l)	Chemotherapy decay rate (gamM)
-50	∞	16.3	16.2	15.9	12.6	17.6	15.7	15.7	15.7	14.5
-40	18.3	16.1	16.1	15.8	13.2	17.1	15.7	15.7	15.7	14.7
-30	16.9	16.0	16.0	15.8	13.7	16.7	15.7	15.7	15.7	15.0
-20	16.2	15.9	15.9	15.8	14.3	16.3	15.7	15.7	15.7	15.3
-10	16.0	15.8	15.8	15.8	15.1	16.0	15.7	15.7	15.7	15.5
0	15.7	15.7	15.7	15.7	15.7	15.7	15.7	15.7	15.7	15.7
+10	15.5	15.6	15.6	15.7	16.5	15.5	15.7	15.7	15.7	15.8
+20	15.3	15.6	15.5	15.6	18.1	15.2	15.7	15.7	15.7	16.0
+30	15.1	15.5	15.5	15.5	27.4	14.8	15.7	15.7	15.7	16.0
+40	14.6	15.5	15.3	15.5	∞	14.5	15.7	15.7	15.7	16.1
+50	14.2	15.4	15.3	15.5	∞	14.1	15.7	15.7	15.7	16.2

Note: ∞ indicates that tumor clearance was not achieved within the 140-day simulation timeframe.

5.6.2. Identification of Sensitive Parameters

Based on the range of variation in tumor clearance time, the parameters were classified into three categories. As illustrated in Figure 22, the tumor growth rate (a) was identified as a highly sensitive parameter, exhibiting the largest impact among all parameters tested. A 30% increase in this parameter extended clearance time from 15.7 to 27.4 days, while a 40% increase prevented clearance within the 140-day simulation timeframe, resulting in a total range of variation of 14.8 days. Sensitive parameters included chemotherapy efficacy (Ks) and the IL-2 killing rate (p1). As shown in Figure 23, chemotherapy efficacy demonstrated a range of 4.1 days; a 50% decrease prevented clearance within the simulation timeframe, whereas a 50% increase reduced clearance time to 14.2 days. The IL-2 killing rate, presented in Figure 24, showed a range of 3.5 days, with a 50% decrease increasing clearance time to 17.6 days and a 50% increase reducing it to 14.1 days.

The chemotherapy decay rate (γ_M) was classified as a moderately sensitive parameter, exhibiting a range of 1.7 days (Figure 24), with clearance time varying from 14.5 to 16.2 days. The remaining parameters—chemotherapy dose, IL-2 injection dose, $CD8^+$ T cell dose, NK cell killing rate (c_n), CD8+ activation rate (J_3), and resistance conversion rate (l)—were classified as insensitive. As demonstrated in Figure 25, these parameters showed minimal variation in clearance time (range ≤ 0.9 days), with clearance time remaining at 15.7 days across all tested variations.

5.5.3. Summary of Sensitivity Findings

The sensitivity analysis revealed that tumor growth rate is the most influential parameter affecting treatment outcome, followed by chemotherapy efficacy and IL-2 killing rate. Parameters related to drug dosing and several immune cell kinetics showed minimal impact under the simulated conditions. The qualitative conclusion that combination therapy with appropriate sequencing outperforms monotherapy remained valid across all parameter variations tested.

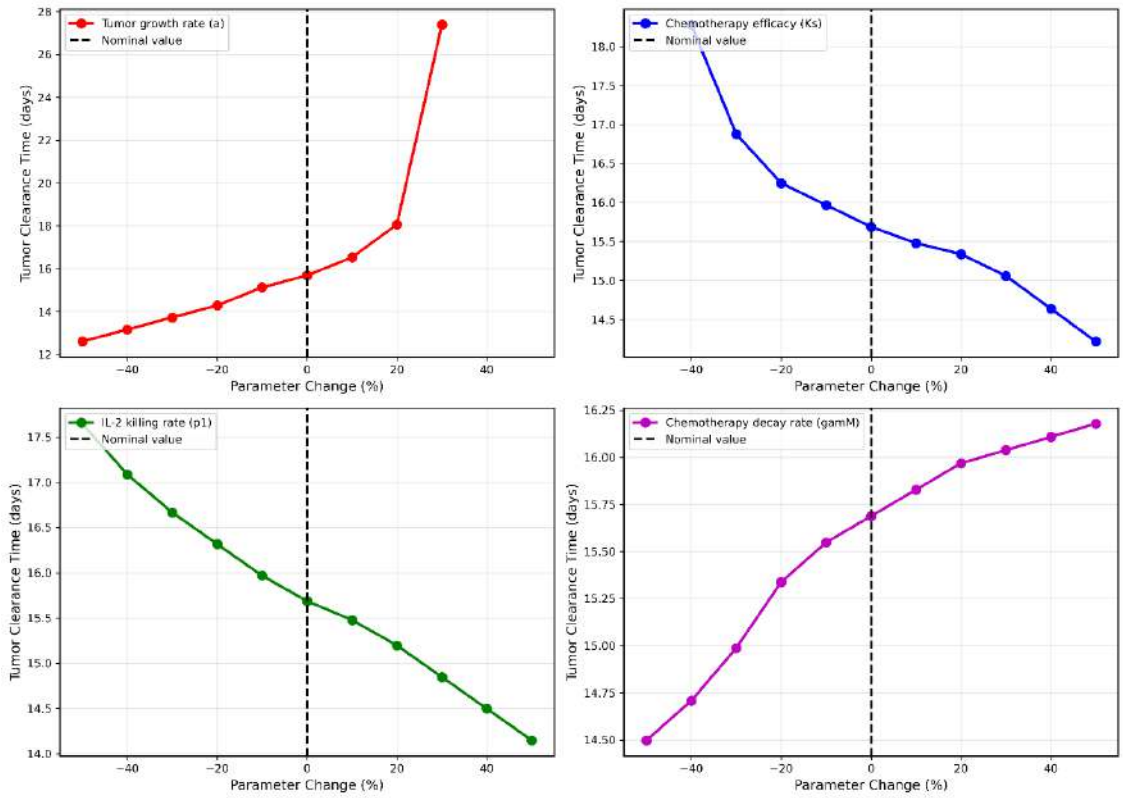


Figure 22: Sensitivity curves for the most influential parameters.

Simulations were conducted using the weak immune system profile with an initial tumor size of 1×10^6 cells. Each panel illustrates the effect of parameter variation (from -50% to +50%) on tumor clearance time for (A) tumor growth rate (a), (B) chemotherapy efficacy (Ks), (C) IL-2 killing rate (p1), and (D) chemotherapy decay rate (γ_M). The vertical dashed line represents the nominal value (0% change). Data points corresponding to parameter variations that did not result in tumor clearance within the 140-day simulation timeframe are omitted from the curves.

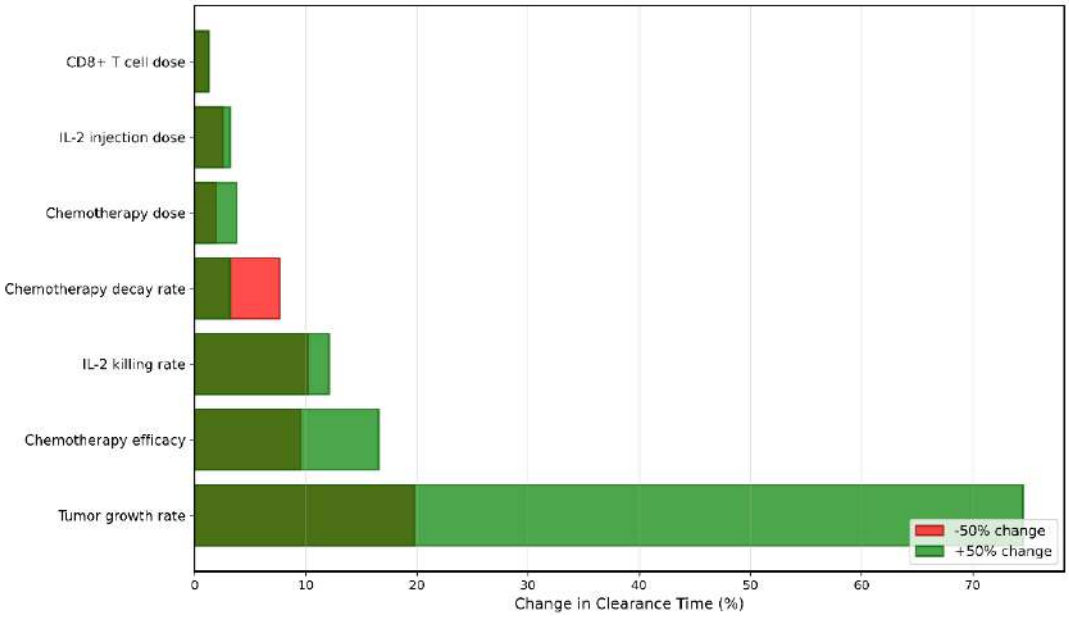


Figure 23: Tornado plot comparing parameter impacts.

Results are based on simulations performed with the weak immune system profile and an initial tumor size of 1×10^6 cells. Bars represent the percentage change in tumor clearance time when each parameter is decreased by 50% (red) or increased by 50% (green) from its nominal value. Parameters are sorted in descending order of influence, with tumor growth rate exhibiting the largest impact. For parameter variations that prevented clearance within the simulation timeframe, the corresponding bars extend to the maximum range shown, as indicated by arrowheads.

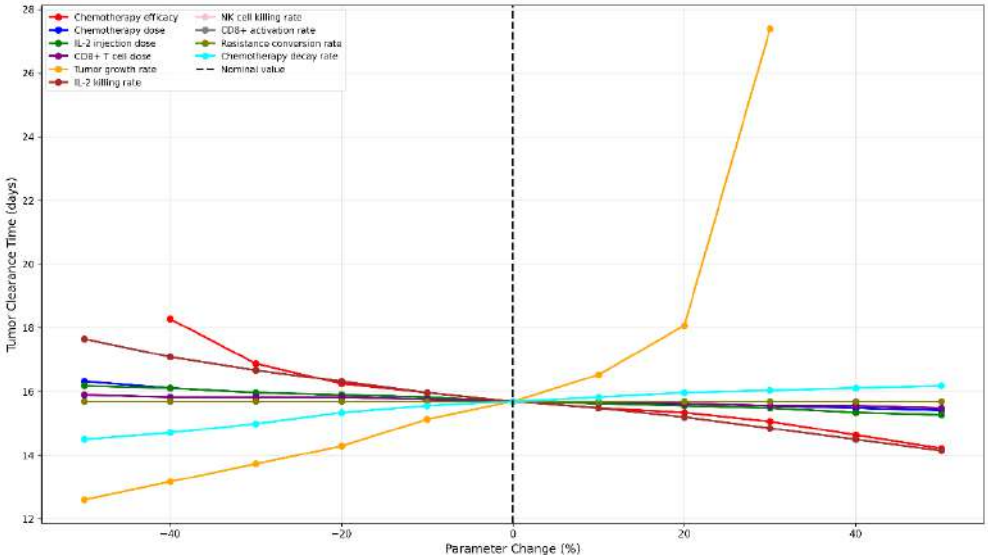


Figure 24: Sensitivity curves for all parameters.

Each line represents the effect of parameter variation on tumor clearance time for one of the eleven parameters analyzed. Simulations were conducted under weak immune conditions with

an initial tumor size of 1×10^6 cells. The vertical dashed line indicates the nominal value (0% change).

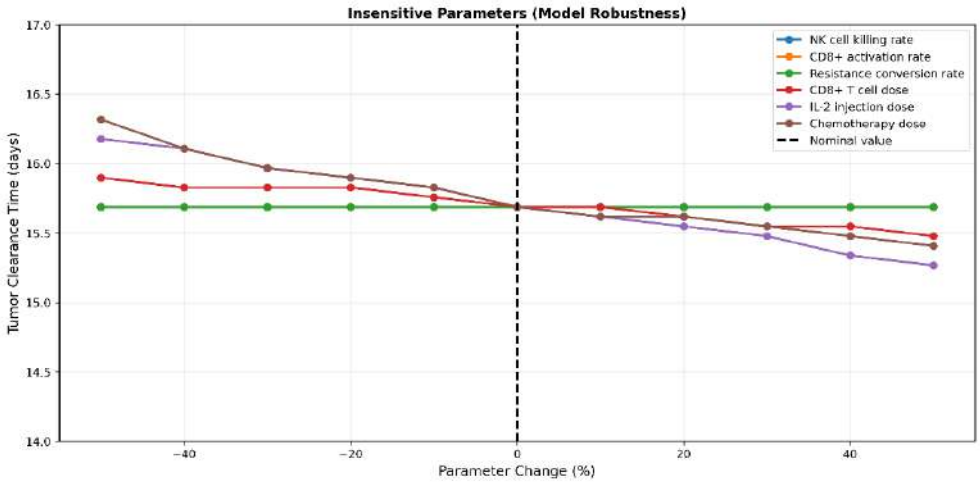


Figure 25: Sensitivity curves for insensitive parameters

Parameters that demonstrated minimal impact on tumor clearance time are presented, including chemotherapy dose, IL-2 injection dose, $CD8^+$T cell dose, NK cell killing rate (c_n), $CD8^+$T activation rate (J_3), and resistance conversion rate (l). Across all variations under the simulated conditions, clearance time remained within a narrow range of 15.4 to 16.3 days.

5.6. Quantitative Comparison of Treatment Strategies

To provide a quantitative assessment of the simulated therapeutic approaches, several performance metrics were extracted from the simulation results. These metrics include tumor clearance time and the minimum level of immune cells during treatment. Table 5 presents a quantitative comparison of all major treatment scenarios.

Table 5: Quantitative comparison of treatment strategies based on simulation results.

Initial Tumor Size	Immune Status	Treatment Protocol	Tumor Clearance Time	Minimum Immune Cell Level	Outcome
1×10^5	Strong	No treatment	Complete	Maintained	Tumor eliminated
1×10^5	Weak	No treatment	Not achieved	Maintained	Tumor growth
1×10^6	Strong	No treatment	Complete	Maintained	Tumor eliminated
1×10^6	Weak	No treatment	Not achieved	Maintained	Tumor growth
1×10^6	Weak	IL-2 immunotherapy (12-day period)	Not achieved	Partially reduced	Partial suppression
1×10^6	Weak	CD8+ T cell injection	Not achieved	Increased	Partial control
1×10^6	Weak	Chemotherapy (10-day cycle)	Approximately day 9	Severely reduced	Elimination with high toxicity
1×10^6	Weak	Chemotherapy (40-day cycle)	Approximately day 11	Low	Elimination with immune damage
1×10^6	Weak	Simultaneous combination	Approximately day 8	Decreased	Elimination with acceptable immunity
1×10^6	Weak	Optimized combination (immune first, chemo day 5)	Approximately day 8	Above 30% of initial	Elimination with preserved immunity
1×10^7	Weak	Chemotherapy (10-day cycle, 3 pulses)	Approximately day 33	Severe drop	Elimination with high risk
1×10^7	Weak	Chemotherapy (10d/4d) + CD8+	Approximately day 20	Improved	Elimination
1×10^7	Weak	Chemotherapy (10d/4d) + CD8+ + IL-2	Approximately day 14	Low in early days	Elimination
1×10^7	Weak	Optimized combination (immune first, chemo day 2)	Day 38	Acceptable	Elimination with preserved health

5.7. Clinical Implications

The simulation results emphasize the clinical significance of treatment sequencing in combined chemo-immunotherapy. According to the model, in patients with small initial tumor size (10^5 cells) and strong immune function, the immune system alone is capable of achieving complete tumor eradication without any therapeutic intervention. However, for larger tumors (10^6 and especially 10^7 cells), particularly when the immune system is weak, monotherapy with either immunotherapy or chemotherapy is insufficient for complete tumor clearance. While chemotherapy alone can significantly reduce tumor burden, it leads to severe suppression of immune cell populations.

In contrast, the optimized combined approach—initiating immunotherapy (IL-2 and $CD8^+$ T cells) first, followed by chemotherapy after a few days—yielded the best outcomes. This strategy achieved complete tumor clearance on day 38 for large tumors (10^7 cells) while preserving immune cell levels above 30 percent of baseline values. These findings indicate that combination therapy outperforms monotherapy particularly when the initial tumor size exceeds 1×10^6 cells or when immune function is compromised. From a clinical perspective, the model suggests that administering immunotherapy prior to chemotherapy may help strengthen the immune system before the introduction of cytotoxic agents, thereby improving treatment efficacy and reducing potential immune-related toxicities in patients with substantial tumor burden.

6. Conclusion

The simulation results suggest that for patients with strong immune status, immune cells alone can eliminate cancer cells without any treatment, while for patients with weak immune status, only very small tumors are eliminated without intervention. For medium and large tumor volumes, therapeutic interventions are necessary to manage and eradicate these cells. From a systems engineering perspective, monotherapy simulations indicate that immunotherapy with interleukin-2 and CD8+ T cells alone cannot completely eliminate cancer cells under the studied parameters. Chemotherapy alone can reduce tumor cell numbers to zero; however, the resulting damage to the immune system significantly lowers the patient’s immunity, posing a serious risk to the system's stability and patient’s health.

To enhance system robustness, a combination of immunotherapy and chemotherapy was investigated. The simulation results indicate that this combination is the most effective among the tested scenarios, provided the treatment sequence is followed. Specifically, immunotherapy must be administered first, followed by chemotherapy, and the scheduling of treatments strongly influences both therapeutic outcomes and the patient’s overall health. Accordingly, depending on tumor size, the optimized sequenced chemo-immunotherapy combination is predicted to be a viable strategy for cancer treatment, achieving complete tumor clearance on day 38 for large tumors while preserving immune cell levels above 30 percent of baseline values. Under the simulated conditions, this framework may function as a model-based decision support system for evaluating complex treatment tradeoffs.

Several limitations of this study should be acknowledged. First, the model has not been quantitatively validated using patient-specific data. While simulation outputs were compared with population-level clinical data from Ghaffari Laleh et al.[16], direct patient-specific calibration was not performed. Second, the model employs ordinary differential equations, which assume homogeneous mixing of cell populations and neglect spatial heterogeneity within the tumor microenvironment. Third, several biological processes were simplified or omitted, including angiogenesis, metabolic constraints, and immune checkpoint dynamics beyond IL-2 signaling. Fourth, the therapy schedules and dosages used in simulations were based on representative protocols from the literature rather than exact clinical protocols from specific

trials. Given these limitations, the results of this study should be interpreted as model-based hypotheses rather than definitive clinical recommendations. Prospective validation using patient-specific data would be required before clinical application.

Future studies are recommended to evaluate the effectiveness of other types of immunotherapy and novel treatment methods in combination with chemotherapy using multi-objective optimization techniques. Additionally, investigations using biological models and simulations that assess the long-term effects of these combined therapies on the immune system and overall patient health could help in developing more efficient and resource-optimized treatment protocols.

7. Nomenclature

7.1. Roman symbols

symbol	definition (unit)
a	Tumor cell intrinsic growth rate
b	Tumor carrying capacity
C	Circulating lymphocyte population
c_n	Tumor cell killing rate by NK cells
d	Half-saturation tumor cell count for $CD8^+$ T cell–mediated killing
e_3	Fraction of circulating lymphocytes differentiating into NK cells
f_2	Natural death rate of NK cells
g_1	Half-saturation constant for tumor killing
g_3	Maximum recruitment rate of NK cells by tumor
g_4	Slope coefficient of NK cell recruitment curve
g_I	Slope coefficient for cytokine-driven $CD8^+$ T cell recruitment
IL_2	Interleukin-2 concentration (IL-2)
J_3	Maximum recruitment rate of $CD8^+$ T cells
K_C	Circulating lymphocyte kill coefficient by chemotherapy
K_N	NK cell kill coefficient by chemotherapy
K_L	$CD8^+$ T cell kill coefficient by chemotherapy
K_S	Tumor cell kill coefficient by chemotherapy
K_3	Slope coefficient of $CD8^+$ T cell recruitment curve
L	$CD8^+$ T cell population
l	Conversion rate of sensitive to resistant tumor cells
l_2	Tumor cell lysis rate by $CD8^+$ T cells
M	Chemotherapy drug concentration
m_1	Natural death rate of $CD8^+$ T cells
NK	Natural killer (NK) cell population
o	Rate constant of $CD8^+$ T cell–mediated tumor lysis term
p_1	Tumor cell killing rate by IL-2
p_a	Inactivation rate of NK cells by tumor cells
P_I	Maximum cytokine-driven recruitment rate of $CD8^+$ T cells
q_l	Tumor-mediated killing rate of $CD8^+$ T cells
R_1	Tumor cell population (treatment-resistant cells)
r_3	Activation rate of $CD8^+$ T cells by NK-mediated tumor cell debris
S	Tumor cell population (treatment-sensitive cells)
u_2	Regulatory suppression of $CD8^+$ T cell proliferation by NK cells
$U_M(t)$	Control function defining the chemotherapy dosing schedule
$V_l(t)$	Control function defining the dosing schedule for $CD8^+$ T-cell immunotherapy
$V_I(t)$	Control function defining the interleukin-2 (IL-2) immunotherapy schedule
Y	$CD4^+$ T cell population

7.2. Greek Letters

symbol	definition (unit)
α	Cytokine production half-saturation constant
α_1	Half-saturation constant for $CD4^+$ T cell production
α_C	Constant source rate of circulating lymphocytes
β_1	Maximum production rate of $CD4^+$ T cells
β_2	Maximum cytokine production rate
β_C	Natural death rate of circulating lymphocytes
γ_M	Chemotherapy drug decay rate
δ	Administered dose of interleukin-2 (IL-2)
δ_2	Tumor-induced death rate of $CD4^+$ T cells
μ_1	Natural death rate of $CD4^+$ T cells
μ_I	IL-2 decay rate
σ	Administered dose of the chemotherapeutic agent
ω	Administered dose of $CD8^+$ T cells

References

1. Tomasetti, C., et al., Only three driver gene mutations are required for the development of lung and colorectal cancers. Proceedings of the National Academy of Sciences, 2015. **112**(1): p. 118-123. https://doi.org/10.1073/pnas.1421839112
2. Vanneman, M. and G. Dranoff, Combining immunotherapy and targeted therapies in cancer treatment. Nature reviews cancer, 2012. **12**(4): p. 237-251. https://doi.org/10.1038/nrc3237
3. Hanahan, D. and R.A. Weinberg, Hallmarks of cancer: the next generation. cell, 2011. **144**(5): p. 646-674. https://doi.org/10.1016/j.cell.2011.02.013
4. Galluzzi, L., et al., Immunological effects of conventional chemotherapy and targeted anticancer agents. Cancer cell, 2015. **28**(6): p. 690-714. https://doi.org/10.1016/j.ccell.2015.10.012
5. Duan, C., et al., Overcoming Cancer Multi-drug Resistance (MDR): Reasons, mechanisms, nanotherapeutic solutions, and challenges. Biomedicine & Pharmacotherapy, 2023. **162**: p. 114643. https://doi.org/10.1016/j.biopha.2023.114643
6. Vafaei, S., et al., Combination therapy with immune checkpoint inhibitors (ICIs); a new frontier. Cancer Cell International, 2022. **22**(1): p. 2. https://doi.org/10.1186/s12935-021-02407-8
7. Lahiri, A., et al., Lung cancer immunotherapy: progress, pitfalls, and promises. Molecular cancer, 2023. **22**(1): p. 40. https://doi.org/10.1186/s12943-023-01740-y
8. Mukherjee, O., et al., Role of chemotherapeutic drugs in immunomodulation of cancer. Current research in immunology, 2023. **4**: p. 100068. https://doi.org/10.1016/j.crimmu.2023.100068
9. Kirschner, D. and J.C. Panetta, Modeling immunotherapy of the tumor–immune interaction. Journal of mathematical biology, 1998. **37**(3): p. 235-252. https://doi.org/10.1007/s002850050127
10. Sudhakar, A., History of cancer, ancient and modern treatment methods. Cancer Science & Therapy, 2009. **1**(02): p. i-iv. https://doi.org/10.4172/1948-5956.100000e2
11. Cai, M., et al., Current therapy and drug resistance in metastatic castration-resistant prostate cancer. Drug Resistance Updates, 2023. **68**: p. 100962. https://doi.org/10.1016/j.drup.2023.100962
12. Khan, S.U., et al., Unveiling the mechanisms and challenges of cancer drug resistance. Cell Communication and Signaling, 2024. **22**(1): p. 109. https://doi.org/10.1186/s12964-023-01302-1
13. Zhang, M., et al., Advances in cancer immunotherapy: historical perspectives, current developments, and future directions. Molecular cancer, 2025. **24**(1): p. 136. https://doi.org/10.1186/s12943-025-02305-x
14. Shu, Y., et al., Mathematical modeling and bifurcation analysis of pro-and anti-tumor macrophages. Applied mathematical modelling, 2020. **88**: p. 758-773. https://doi.org/10.1016/j.apm.2020.06.042
15. Pang, L., et al., Mathematical modeling and analysis of tumor-volume variation during radiotherapy. Applied Mathematical Modelling, 2021. **89**: p. 1074-1089. https://doi.org/10.1016/j.apm.2020.07.028
16. Ghaffari Laleh, N., et al., Classical mathematical models for prediction of response to chemotherapy and immunotherapy. PLoS computational biology, 2022. **18**(2): p. e1009822. https://doi.org/10.1371/journal.pcbi.1009822
17. Sung, P.W., et al., Mathematical modeling to simulate the effect of adding radiation therapy to immunotherapy and application to hepatocellular carcinoma. International Journal of Radiation Oncology* Biology* Physics, 2022. **112**(4): p. 1055-1062. https://doi.org/10.1016/j.ijrobp.2021.11.008
18. Kim, Y., et al., A mathematical model for predicting patient responses to combined radiotherapy with CTLA-

4 immune checkpoint inhibitors. Cells, 2023. **12**(9): p. 1305. https://doi.org/10.3390/cells12091305
19. Bitsouni, V. and V. Tsilidis, Mathematical modeling of tumor-immune system interactions: the effect of rituximab on breast cancer immune response. Journal of Theoretical Biology, 2022. **539**: p. 111001. https://doi.org/10.1016/j.jtbi.2021.111001
20. Al-Haideri, M., et al., CAR-T cell combination therapy: the next revolution in cancer treatment. Cancer cell international, 2022. **22**(1): p. 365. https://doi.org/10.1186/s12935-022-02778-6
21. Mahasa, K.J., et al., A combination therapy of oncolytic viruses and chimeric antigen receptor T cells: a mathematical model proof-of-concept. Mathematical Biosciences and Engineering, 2022. **19**(5): p. 4429-4457. https://doi.org/10.3934/mbe.2022205
22. Shariatpanahi, S.P., et al., Mathematical modeling of tumor-induced immunosuppression by myeloid-derived suppressor cells: Implications for therapeutic targeting strategies. Journal of theoretical biology, 2018. **442**: p. 1-10. https://doi.org/10.1016/j.jtbi.2018.01.006
23. Owens, K. and I. Bozic, Modeling CAR T-cell therapy with patient preconditioning. Bulletin of Mathematical Biology, 2021. **83**(5): p. 42. https://doi.org/10.1007/s11538-021-00869-5
24. de Pillis, L.G., W. Gu, and A.E. Radunskaya, Mixed immunotherapy and chemotherapy of tumors: modeling, applications and biological interpretations. Journal of theoretical biology, 2006. **238**(4): p. 841-862. https://doi.org/10.1016/j.jtbi.2005.06.037
25. Van Eijk, M., J.H. Beijnen, and A.D. Huitema, Time above threshold plasma concentrations as pharmacokinetic parameter in the comparison of oral and intravenous docetaxel treatment of breast cancer tumors. Anti-Cancer Drugs, 2023. **34**(2): p. 281-289. https://doi.org/10.1097/CAD.0000000000001426



This article is an open-access article distributed under the terms and conditions of the Creative Commons Attribution (CC-BY) license.